

Dempster-Shafer Theory Based Cooperative Energy Detection Under Noise Uncertainties In Cognitive Radio Networks

Thesis submitted in partial fulfillment
of the requirements for the degree of

Master of Science
in
Electronics and Communication Engineering

by

Prakash Borpatra Gohain

201432659

prakash.gohain@research.iiit.ac.in



Signal Processing and Communication Research Center (SPCRC)

International Institute of Information Technology

Hyderabad - 500 032, INDIA

December 2017

Copyright © Prakash Borpatra Gohain, 2017
All Rights Reserved

International Institute of Information Technology
Hyderabad, India

CERTIFICATE

It is certified that the work contained in this thesis, titled “Dempster-Shafer Theory Based Cooperative Energy Detection Under Noise Uncertainties In Cognitive Radio Networks” by Prakash Borpatra Gohain, has been carried out under my supervision and is not submitted elsewhere for a degree.

Date

Adviser: Dr. Sachin Chaudhari

To
My Family and Friends...

Acknowledgments

The three years I spent in IIIT-H have been a wonderful and great learning experience. Before stepping into IIIT-H, my knowledge of how to conduct good quality research was very limited and unpolished. But with good guidance, support and hard work my understanding of research took a new turn and I have started loving it more than before. As I submit my MS thesis, I wish to extend my gratitude to all those people who helped me in successfully completing this phase of my life.

First and foremost I would like to offer my deepest gratitude to my advisor Dr. Sachin Chaudhari. For me he is an embodiment of hard work, patience and dedication. His guidance, insight, knowledge and support were invaluable to me throughout my entire MS journey. He has played the most important role in shaping my personality and moulding my thoughts in the right direction. The discussions I had with him on a daily basis have helped me grow immensely, both as a person as well as a researcher.

I am also extremely grateful to Prof. Visa Koivunen with whom I had the privilege of co-authoring two papers in this thesis. I thank him for providing healthy comments and suggestions, which helped us to further polish both the technical as well as the theoretical aspects of the papers.

I am thankful to Center for Excellence in Signal Processing (CESP) and Science and Research Board (SERB), Department of Science and Technology (DST), India, for providing me financial support during my MS tenure.

Further, I am thankful to all my colleagues and friends in SPCRC for providing a positive work environment. Special thanks to Upendar, Rhishi, Nachiket, Pratik, Mahesh, Maneesh, Deepa, Kunal, Sumit, Rakesh, Anish, Shivakrishna, Hari, Vaishali, Prateek, Shastri and Irshad for being an integral part of my life at IIIT-H. The fun-filled moments that we shared together, will always stay with me forever. Also, many thanks to Sailaja madam for her help in all the office related works.

Last but not the least, I am thankful to my family for believing in me and supporting me in every way possible to fulfill my dreams.

Abstract

Obtaining awareness about the state of the spectrum via sensing is crucial in many systems including cognitive radio (CR), cognitive radars, automotive sensing and communication where spectrum sharing is required. In the context of CR, spectrum sensing is a key enabler for obtaining spectrum awareness, which detects the activity of a licensed user or primary user (PU) in a particular band of interest to provide opportunistic usage of spectrum to the secondary users (SUs).

In this thesis, we focus on cooperative energy detection (CED) in a CR network. CED is a distributed detection scheme where all the SUs employing energy detector (ED), collaborate to perform spectrum sensing to identify spectrum holes. A centralized soft combining approach is considered such that the SUs send the energy value, calculated from the received signal, to the fusion center (FC). Using sum fusion rule and Neyman-Pearson (NP) criterion, the FC makes the global decision of whether the frequency band is occupied by the PU or not. However, implementing CED requires knowledge of noise variance (noise power) for setting the threshold. But in real world scenario, noise variance may change due to several reasons such as temperature, external interference, etc. As a result, slight change or deviation of noise variance from the assumed value leads to unpredictable performance in CED. Moreover, in the presence of noise uncertainty (NU), CED suffers from performance limitation in the form of signal-to-noise-ratio (SNR) wall. SNR wall phenomenon in CED has been well investigated in literature but only considering homogeneous CR nodes having same NU parameters. In this thesis, we extend the concept of SNR wall in CED to a more general case by considering that all the participating SUs have different NU parameters. The generalized SNR expression for this case is derived and a new terminology called “signal power wall (SP wall)” is defined to explain the concept of SNR wall in this heterogeneous CR network.

Handling NU in CED using traditional probabilistic methods have not borne any fruits beyond certain thresholds, which forced us to look for concepts and theories beyond standard Bayesian approach. In this context, *Dempster-Shafer theory* (DST) (also called *evidence theory*) provides a new dimension to the picture. It enables us to include uncertainty or ignorance as a quantity in the fusion process. The theory has the ability to quantify our lack of knowledge or how much we are uncertain about something, instead of ignoring them altogether. Using the tools of evidence theory, we forged a new CED algorithm for spectrum sensing under NU. In the proposed scheme, the SUs send basic mass assignment (BMA) values or *belief values* to the FC, instead of the energy values. A novel method to compute the BMA values based on energy of the received signal is proposed. The uncertainty in noise variance is accounted

by discounting the BMA values of each SU by the amount of trust associated with the SU, where the trust factor is inversely proportional to the amount of NU present in the SU. At the FC, Dempster combination rule is applied to fuse these discounted BMA values. Even in this case, NP criterion is employed for designing the detector at the FC. The final test statistic is compared with the predefined threshold (based on NP criterion) to make the global decision. Extensive simulation results have shown that the proposed DST based CED scheme is able to surpass the traditional soft combining based CED scheme and is also successful in lowering the SNR/SP wall barrier of CED.

Contents

Chapter	Page
1 Introduction	1
1.1 Motivation	1
1.2 Thesis overview	3
1.3 Why the theory of evidence?	4
1.4 Related work	4
1.5 Contribution of the thesis	4
1.6 Thesis outline	5
2 Cognitive Radio - A Brief Overview	7
2.1 Definition	7
2.2 Dynamic spectrum access	8
2.3 Spectrum sensing	9
2.3.1 Techniques	10
2.3.2 Performance criteria	11
2.3.3 Detection criteria	13
2.4 Cooperative spectrum sensing	15
2.4.1 Classification and framework of CSS	15
2.4.2 Hard decision combining	16
2.4.3 Soft combining	17
3 Sum Fusion Rule based CED and Generalized SNR Wall	18
3.1 System model for sum fusion based CED	19
3.2 Effect of NU	22
3.2.1 NU models	22
3.2.2 Sum fusion rule under NU	24
3.3 SNR wall	25
3.4 Generalized SNR wall	25
3.4.1 SNR wall as a special case of SP wall	26
3.5 SP wall analysis and comparison in sum rule based CED	27
4 Dempster-Shafer Theory of Evidence	30
4.1 Frame of discernment	31
4.2 Basic mass assignment	31
4.3 Belief functions	33
4.4 Commonality numbers	34

4.5	Degrees of doubt and upper probabilities	34
4.6	Bayesian belief function	35
4.7	Dempster rule of combination	36
4.8	Illustration	37
5	Dempster-Shafer Theory based Cooperative Energy Detection Scheme	44
5.1	Proposed scheme under unknown but constant noise variance	44
5.1.1	Proposed BMA method	45
5.1.2	BMA adjustment under NU	48
5.1.3	Determining discount rate α_i	49
5.1.4	Data fusion at the FC	50
5.1.5	Optimality of the proposed scheme in the absence of NU	51
5.2	Simulation results under unknown but constant noise variance	52
5.2.1	Performance analysis of the proposed DST scheme	53
5.2.2	Performance comparison of DST and sum fusion rule	53
5.2.2.1	Homogeneous SUs	53
5.2.2.2	Heterogeneous CR nodes	54
5.3	Proposed DST based CED under random noise variance	56
5.3.1	BMA method under random noise variance	56
5.3.2	BMA adjustment under NU	58
5.3.3	Determining discount rate α_i under random noise variance	58
5.3.4	Data fusion at the FC	60
5.4	Simulation results under random noise variance	60
5.5	Comparison between DST and sum in terms of SNR and SP walls	62
6	Conclusion	64
	Bibliography	67

List of Abbreviations

5G	fifth generation
BMA	basic mass assignment
CR	cognitive radio
CED	cooperative energy detection
CSS	cooperative spectrum sensing
D2D	device to device
DSA	dynamic spectrum access
DST	Dempster-Shafer theory
ED	energy detector
FC	fusion center
FCC	Federal Communications Commission
GSM	global system for mobile communications
IoT	Internet of things
LTE	long term evolution
M2M	machine to machine
NP	Neyman-Pearson
NTIA	National Telecommunications and Information Administration
NU	noise uncertainty
OFDM	Orthogonal Frequency Division Multiplexing
PU	primary user
QoS	Quality of Service
SNR	signal-to-noise-ratio
SP	signal power
SU	secondary user
TRAI	Telecom Regulatory Authority of India
WiMax	worldwide interoperability for microwave access

List of Symbols

α_i	Discount rate for the i^{th} SU
$\bar{\eta}_{sum}$	Threshold at the FC for sum rule under NU (random variable model)
β	False alarm constraint at the FC
Δ_i	Noise deviation in dB for the i^{th} SU
η'_{sum}	Threshold at the FC for sum rule under NU (unknown constant model)
η_{ds}	Threshold at the FC under DST rule
η_i	Threshold at the i^{th} SU
η_{sum}	Threshold at the FC under sum rule
$\hat{m}_i(\cdot)$	Discounted BMA function for the i^{th} SU
μ_0	Mean of T_{sum} under H_0
μ_1	Mean of T_{sum} under H_1
μ_{0i}	Mean of energy under H_0 at the i^{th} SU
μ_{1i}	Mean of energy under H_1 at the i^{th} SU
ρ_i	Noise uncertainty factor at i^{th} SU
σ_0^2	Variance of T_{sum} under H_0
σ_1^2	Variance of T_{sum} under H_1
σ_i^2	True noise variance at the i^{th} SU
σ_{0i}^2	Variance of energy under H_0 at the i^{th} SU
σ_{1i}^2	Variance of energy under H_1 at the i^{th} SU
σ_{li}^2	Upper bound on noise variance for the i^{th} SU

σ_{ni}^2	Nominal noise variance for the i^{th} SU
σ_{ui}^2	Upper bound on noise variance for the i^{th} SU
$\text{SNR}_n(\text{dB})$	Nominal signal-to-noise-ratio in dB
$\text{SNR}(\text{dB})$	True signal-to-noise-ratio in dB
SNR	True signal-to-noise-ratio
SNR_{wall}	Signal-to-noise-ratio wall
SNR_n	Nominal signal-to-noise-ratio
SP_{wall}	Signal power wall
E_i	Received signal energy
H_0	Null Hypothesis
H_1	Alternate Hypothesis
$M(\cdot)$	Total combined basic mass value
$m_i(\cdot)$	BMA function for the i^{th} SU
N	Received signal sample size
P	Average PU signal power
P'_d	Average probability of detection
P'_{fa}	Average probability of false alarm
P_d	Probability of detection
P_{di}	Probability of detection at the i^{th} SU
P_{fa}	Probability of false alarm
P_{fi}	Probability of false alarm at the i^{th} SU
$Q(\cdot)$	Tail probability of normal distribution
T_{ds}	DST rule based test statistic at the FC
T_{sum}	Sum rule based test statistics at the FC
U	Number of SUs

List of Figures

Figure	Page
1.1 Spectrum allocation chart for the United States [2].	2
1.2 Figure shows the basic concept of opportunistic access of spectrum holes by the CR users [11]. A CR senses the spectrum for occupancy by PUs, and transmits its data only when the frequency band is unused.	2
2.1 DSA consists of three important functions: spectrum awareness, cognitive processing and spectrum access [7].	8
2.2 Classification of spectrum sensing schemes [50].	10
2.3 Basic block diagram of an ED [57].	11
2.4 Figure showing probability of false alarm (P_{fa}) and probability of miss detection (P_m) with threshold η	12
2.5 Framework for centralized CSS structure. For hard decision combining each SU sends its one bit local decision D_i to the FC. In the soft combining approach, the SUs sends their corresponding test statistic, T_i to the FC. The FC reports back the global decision to all the SUs.	16
3.1 Considered CED model: SUs have non-identical NU parameters. Each SU evaluates energy from the observed data and sends it to the FC, where sum fusion rule is applied for decision making.	19
3.2 (a) Distribution of $2E_i/\sigma_i^2$ for $N = 5$ and $\text{SNR} = -5$ dB. (b) Asymptotic distribution of E_i for $N = 500$ and $\text{SNR} = -10$ dB.	21
3.3 Sample size N (in log scale) vs average signal power, P for case I, II, III and IV.	28
4.1 Measure of Bel, Pl and their complements along with the concept of uncertainty [28].	35
5.1 Framework for the proposed DST based CED.	45
5.2 Plot of α_i for different NU intervals as a function of β_i , $\text{SNR}_n(\text{dB}) = -5$ dB and $N = 300$ for different values of noise uncertainty interval Δ	50
5.3 P_d vs $\text{SNR}_n(\text{dB})$ plots of DST scheme for homogeneous case with different number of SUs in the presence ($\Delta = 0.5$ dB) and absence ($\Delta = 0$ dB) of NU. Here, $\beta_i = \beta = 0.1$	52
5.4 (a) ROC curves for the proposed DST based CED for homogeneous case considering different number of participating SUs in the presence ($\Delta = 0.5$ dB) and absence ($\Delta = 0$ dB) of NU at $\text{SNR}_n(\text{dB}) = -6$ dB. (b) Zoomed portion of figure (a).	53

5.5 (a) P_d vs $\text{SNR}_n(\text{dB})$ comparison between the proposed DST and the sum fusion rule for CED with homogeneous SU nodes. Here $U = 3$ and $\beta = 0.1$. (b) Comparison of ROCs for DST and sum based CED schemes for $\text{SNR}_n(\text{dB}) = -6$ dB under homogeneous NU parameters $\Delta = 0, \Delta = 0.5$ dB, with $\sigma_n^2 = 1$ and number of SU, $U = 3$ 54

5.6 (a) P_d vs P (log scale) comparison for CED under generalized heterogeneous NU parameters. (b) ROC Comparison of DST and sum based CED schemes for average signal power, $P = 0.3$ under generalized heterogeneous NU parameters. 55

5.7 (a) P_d vs $\text{SNR}_n(\text{dB})$ plot of sum fusion rule for different values of σ_i^2 . (b) P_d vs $\text{SNR}_n(\text{dB})$ plot of DST fusion rule for different values of σ_i^2 . σ_L^2 denotes the lower limit of noise variance and σ_U^2 the upper limit. 55

5.8 Framework for the proposed DST based CED. 56

5.9 The discounting rate α_i , as a function of constraint on the false alarm probability for $\text{ASNR}(\text{dB}) = -10$ dB. For $\beta_i = \beta = 0.1$, the discount rate α_i is the point where the dotted line intersects the α_i curve. 59

5.10 (a) P'_d as a function of $\text{ASNR}(\text{dB})$ for $\beta = 0.1$ considering σ_w^2 as a Gaussian distributed random variable. (b) ROC curves comparison at $\text{ASNR}(\text{dB}) = -10$ dB considering σ_w^2 as a Gaussian distributed. 61

5.11 (a) P'_d as a function of $\text{ASNR}(\text{dB})$ for $\beta = 0.1$ considering σ_w^2 as a uniformly distributed random variable. (b) ROC curves comparison at $\text{ASNR}(\text{dB}) = -10$ dB considering σ_w^2 as a uniformly distributed random variable 61

5.12 Comparison of the DST and sum fusion rules in terms of sample size N as a function of P and $\text{SNR}_n(\text{dB})$ with NU parameters corresponding to cases I and III in Table 5.1 with $\sigma_{ni}^2 = \sigma_n^2$ 62

5.13 Comparison of the DST and sum fusion rules in terms of sample size N as a function of P for scenarios corresponding to cases II and IV in Table 5.1. 63

List of Tables

Table	Page
3.1 The considered heterogeneous cases of NU.	28
3.2 SP wall: theory vs simulated.	29
4.1 Interpretation of elements of 2^{Θ}	37
4.2 Basic mass assignment to different subsets of the power set by the two detectives	38
4.3 Table showing the values for m , Bel, Pl, and Dou of different elements for both detectives.	39
4.4 Cut set table	39
4.5 The reduced combinable table	40
4.6 The product table	41
4.7 The basic mass assignment and the related evidence measures <i>belief, plausibility, commonality, doubt</i> and <i>uncertainty</i>	42
5.1 Considered cases for SP wall simulation and comparison between DST and sum rule CED.	62

Chapter 1

Introduction

1.1 Motivation

The world of wireless communication is heavily dependent on the radio frequency spectrum, which is one of the most tightly regulated resources of all time. Spectrum usage by the legalized users' needs to follow specific rules and regulations put forward by the regulatory bodies. In the United States, the Federal Communications Commission (FCC) regulates interstate and international communications by radio, television, wire, satellite and cable under a command-and-control model [1]. The FCC allocates frequency bands to be exclusively used for a particular service within a given spatial region and for a specified time duration. Similarly, in India, Telecom Regulatory Authority of India (TRAI) is the government regulatory body that allocates spectrum to different technologies. Figure 1.1 shows the National Telecommunications and Information Administration (NTIA) chart of spectrum allocation in the United States [2]. It is evident from the chart that most of the frequencies are already allocated, and there is very little room for new and innovative services in the future.

With the expansion in the number of wireless gadgets, several new top of the line applications and the regularly expanding demand for higher data rates have put a toll on the radio frequency spectrum. Also, with the approach of technologies like Internet of things (IoT) [3, 4], device to device (D2D) and machine to machine (M2M) communications [5, 6], billions of wireless devices performing easy to complicated tasks will be added to the already existing crowded wireless spectrum. Subsequently, accessibility of good quality wireless spectrum will be a major bottleneck for such future wireless applications. However, real measurements performed in different nations demonstrate that the greater part of the radio frequency range is wastefully used with frequency usage generally in the scope of 5%-50%. Therefore, the genuine issue is not spectrum shortage but rather the wasteful or inefficient frequency utilization. This inefficiency comes about because of static spectrum allotments, inflexible regulations, rigid radio capacities, and constrained network coordination [7]. In such a scenario, opportunistic spectrum access provided by cognitive radio (CR) will enable these devices to efficiently use the spectrum and enhance reliability in data transfer [8, 9, 10]. CR offers the possibility to significantly increase the spectrum efficiency by smart secondary users (SUs) utilizing the licensed user or primary user (PU)

Spectrum sensing is a key facilitator for flexible spectrum use in CRs as it provides spectrum awareness crucial for maximizing the spectrum utilization while restricting the interference to the PU to minimum [17, 18]. This makes spectrum sensing one of the fundamental blocks in the operation of a CR. Moreover, obtaining awareness about the state of the spectrum via sensing, is also crucial in many other systems such as cognitive radars, automotive sensing and communications where spectrum sharing is required. Thus, spectrum sensing is the first step towards spectrum sharing.

In the context of spectrum sensing for CR networks, cooperative energy detection (CED) is an attractive choice because of its simplicity, low power consumption and ability to capture highly dynamic behavior of radio spectrum [19, 20]. It is basically a cooperative spectrum sensing scheme where several energy detection based CRs collaborate to detect the PU activity in a given spectrum. It also has good sensing performance when noise variance or noise power is exactly known [21, 22]. However, the noise variance present in our observations is unknown and has to be estimated. As with the estimates of system parameters in real physical world, these estimates are also subjected to uncertainty. Typically the uncertainty in noise variance is ± 1 dB even if the impact of external interference is excluded. If interferences are taken into account, the uncertainty can be significantly higher [23]. In the presence of noise uncertainty (NU), detection schemes based on the energy of the observed signal suffer from drastic performance degradation as well as from the performance limitation of SNR wall as was shown for local detector in [24] and for cooperative sensing in [25, 26].

1.2 Thesis overview

The primary focus of this thesis is to discuss the effects of NU in CED and to design a new cooperative detection scheme based on Dempster-Shafer theory (DST) also called evidence theory to handle this issue of NU. Generally, if we consider a group of CR based sensor nodes performing CED to detect a PU activity, the NU parameters of all sensors can be identical or they can be dissimilar for each sensor. In this context, NU parameters refers to the parameters that define the NU model. However, it is very unlikely that each of these SUs would have exactly the same NU parameters. Therefore, we take into account this factor of heterogeneity in our model of CED, where we consider each SU to have its own unique NU parameters. Moreover, this idea of heterogeneity makes the model more universal since all other combinations of NU parameters can be derived from it including the special case of homogeneous, i.e. all the CR nodes have exactly the same NU parameters.

The first part of the thesis deals with the SNR wall formation in the case of CED under NU considering heterogeneous CR nodes, i.e., nodes with different NU parameters. We introduce a new term called *signal power wall* or SP wall, which can be considered as a generalized form of SNR wall in CED with heterogeneous CR nodes. In the second part of this thesis, two novel DST based CED schemes are proposed. These two schemes vary based on the noise variance model used. The proposed schemes takes into account the NU present in CED and is able to enhance the sensing performance of the CR network.

1.3 Why the theory of evidence?

Currently in spectrum sensing literature, design of most of detectors including the sum fusion rule is based on the Bayesian probability theory. One drawback of the Bayesian probability theory is its inability to deal with any uncertainty in the observed data. DST, also referred to as *evidence theory* or *theory of belief functions*, has the ability to mathematically represent uncertainty or ignorance [27]. Confidence values in DST are associated to the elements of the power set 2^Θ instead of Θ as in the probability theory. This allows for modeling ignorance and uncertainty in the observed data. The theory can also provide an upper and lower bound on the likelihood of an event. Moreover, the theory provides Dempster's rule of combination for fusing data from various independent sources. As such, it has been widely used in several applications including safety-and-reliability modeling, artificial intelligence, object classification, target tracking, information fusion, process engineering. See [27, 28, 29, 30] for more details. In this thesis, we propose the use of DST as an efficient alternative to the traditional sum fusion rule [31] for CED in the presence of NU.

1.4 Related work

Evidence theory or DST has been applied earlier to the problem of distributed detection in traditional networks [32] while in CR networks, it has been applied to CED in [33, 34, 35]. In [33], SU's credibility was evaluated based on the imperfections in the decisions at the SU arising out of the channel conditions between the PU and the SU. In [34], it is assumed that SNR values at SUs are different and credibility for each SU is calculated to evaluate the degree of reliability of each local spectrum sensing terminal. The work in [34] is later extended in [35] by employing an effective quantizer for the sensing data based on the hypothesis distribution under different signal-to-noise ratios (SNRs) of the PU signal. However, the works in [33, 34, 35] assume that the noise variance is perfectly known while in our work we specifically targets the scenario where there is uncertainty in the noise variance at each SU. There are few papers [36, 37] which have tried to improve the performance of CED in the presence of NU. However, the work in [36, 37] do not employ DST which is the prime focus of this thesis.

1.5 Contribution of the thesis

The contributions of this thesis are as follows:

- The concept of generalized SNR wall for CED, with SUs having heterogeneous NU parameters is proposed. The expressions for generalized SNR wall, which has been termed as *signal power wall (SP wall)* are derived for the sum fusion rule, which is a well-known soft combining technique for CED [31]. Also, the idea of heterogeneous SU in the CR network, provides a new insight in the performance of the CED for PU signal detection.

- Two novel DST based CED schemes under NU with heterogeneous CR nodes are proposed based on two noise variance models considered in this thesis. In the first DST scheme, the noise variance is modeled as a unknown but deterministic constant. Here, the true noise variance lies within a lower and upper bound. These bounds define the NU interval. In the second DST scheme, noise variance is modeled as a random variable with a known distribution.
- In both the proposed DST based CED schemes, the SUs evaluates the basic mass assignment (BMA) values or belief values for each SU based on the likelihood functions of the energies, evaluated from the received observations. In the presence of NU, the effect of NU is taken into consideration by discounting the BMA of each sensor node. A method is proposed to evaluate the discount factor based on the range of uncertainty in the noise variances. Each SU sends its discounted BMA values to the fusion center (FC) which fuses them using Dempster combination rule.
- It is shown that when there is no uncertainty in the noise variance, the Dempster combination rule based on the proposed BMA, boils down to the optimal fusion rule of likelihood ratio under the assumption of conditional independence of observations at the SUs. In the presence of NU, the detection performance of the proposed DST based CED is superior and improved compared to the traditional sum fusion rule under both the considered noise variance models.
- Finally, SP wall (generalized SNR wall) values for DST and sum rule based CED are simulated and compared, which also demonstrated that the proposed scheme is able to lower the SNR wall barriers possessed by sum fusion rule.

1.6 Thesis outline

Chapter 2 provides an overall overview of CR and its related topics. Starting with the basic definitions, we move towards dynamic spectrum access (DSA), different state-of-the-art spectrum sensing techniques. Towards the end of the chapter, the need of cooperative spectrum sensing (CSS) in CR is discussed and different types of CSS schemes are explained.

In chapter 3, the CED based on the sum fusion rule is introduced and explained in detail. Next, the concept of NU is discussed, how NU is modeled and its effects on threshold evaluation and detection performance in case of sum fusion rule is explained. Finally, we talk about formation of SNR wall in CED under NU and propose the generalized SNR termed as SP wall, considering heterogeneous CR nodes.

In chapter 4, a detailed explanation regarding the basics of DST is provided. Although DST has been used by researchers and theorists in many different fields and subjects, it has not been explored much in the field of wireless communications. Hence, some preliminary knowledge is required to understand the later part of the thesis since the prime focus of this thesis is developing a detection scheme based on DST.

Chapter 5 presents the proposed DST based CED scheme in CR network with heterogeneous SUs. It consists of two DST based CED schemes depending on the NU model used. Next, simulation results are presented showing comparison of proposed scheme to the traditional sum fusion rule based CED.

Finally, chapter 6 concludes the thesis with some future work involving DST.

Chapter 2

Cognitive Radio - A Brief Overview

A typical radio system has fixed operating parameters such as frequency of operation, modulation technique used, protocol, networking, etc. The drawback of having fixed parameters is that it leads to static behavior and the radio fails to maximize its performance in different scenarios. In this regard, the concept of CR can play a very significant role in changing the way radios work and bring out a whole new definition of radio that can perform in a dynamic and intelligent fashion, thus maximizing its performance. The vision of CR technology is to make the existing radio technology smart. A smart radio will have the capability to learn services available in locally available wireless networks. A CR could interact with those networks in their preferred protocols so that there is no confusion in finding the perfect wireless network for a particular operation. Additionally, it could use the frequencies and choose waveforms that minimize and avoid interference with existing radio communication systems [38].

2.1 Definition

The term “cognitive radio” was initially coined by Mitola in the late 1990’s [39, 40] as an *intelligent radio which is aware of its surrounding environment and capable of changing its behavior to optimize the user experience*. Slightly different CR characterizations are given in [41, 42]. However, the formal definition of CR as given by FCC is [43]:

Cognitive Radio is a radio or system, that senses its operational electromagnetic environment and can dynamically and autonomously adjust its radio operating parameters to modify interference, facilitate interoperability, and access secondary markets.

In the context of CR networks there are basically two types of users. They are described as follows:

- **Primary user (PU):** These wireless devices are the primary license-holders of the spectrum band of interest. In general, they have priority access to the spectrum, and subject to certain Quality of Service (QoS) constraints which must be guaranteed. Some examples of licensed technology are global system for mobile communications (GSM) [44], worldwide interoperability for microwave access (WiMax) [45], and long term evolution (LTE) [45].

- **Secondary user (SU):** These users may access the spectrum, which is licensed to the PUs. Thus, they are SUs of the wireless spectrum, and are basically considered to be CRs. For the rest of this thesis, we will assume that the SUs are CRs and will use the terms interchangeably. These SUs employ their “cognitive” abilities to communicate while ensuring the communication of the PUs is kept at an acceptable level [46].

2.2 Dynamic spectrum access

A SU can access spectral resources of a PU when the PU is idle. However, the moment the PU becomes active the SU has to immediately vacate the frequency band such that minimal or no interference is caused to the PU. Such opportunistic access of the PU resources by the SUs is called as **dynamic spectrum access (DSA)** [47]. The main functions of DSA are [11]

- **Spectrum awareness**
- **Spectrum access**
- **Cognitive processing**

Fig. 2.1 shows the functions involved in DSA and how they coordinate among themselves [7].

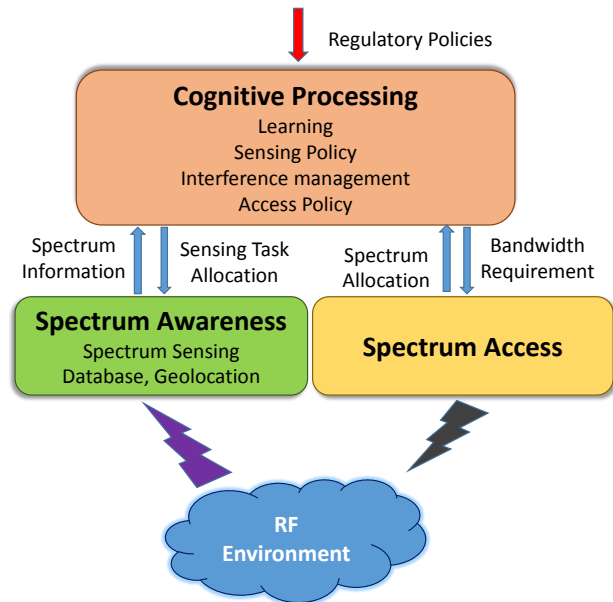


Figure 2.1: DSA consists of three important functions: spectrum awareness, cognitive processing and spectrum access [7].

Spectrum awareness generates awareness about the frequency spectrum. Spectrum awareness can be obtained in two ways by using either active or/and passive methods. In the active method or spectrum

sensing, the radios become spectrum aware by detecting and estimating the spectrum. Active methods have broader application areas and lower infrastructure requirement. In passive methods, the information regarding the unoccupied spectrum is provided to the SU [48].

Spectrum access also called spectrum sharing, offers techniques to take advantage of the existing spectrum opportunities for efficient reuse. Spectrum sharing process consists of the following steps namely: spectrum allocation, spectrum access, transmitter-receiver handshake and spectrum mobility [49].

Cognitive processing is the intelligence and decision making function which includes quite a few sub-tasks such as learning about the radio environment, designing efficient sensing, and access policies alongside managing interference for coexistence of the SU and PU systems [39].

As the focus of this thesis is on spectrum sensing, we present the concepts related to spectrum sensing in detail in the next section.

2.3 Spectrum sensing

Spectrum sensing in the context of CR can be defined as the detection of the presence or absence of PU signal in a given frequency band of interest. The basic concept of spectrum sensing is modeled as a binary hypothesis testing problem between the noise-only hypothesis and the signal-present hypothesis. In classical detection theory, these two hypotheses of noise-only and signal-present are termed as null hypothesis and alternate hypothesis respectively. The null hypothesis is denoted as H_0 and the alternate hypothesis is denoted as H_1 . The observations $x[n]$ under H_0 and H_1 can be expressed as

$$\begin{aligned} H_0 : x[n] &= \text{noise}[n] \\ H_1 : x[n] &= \text{signal}[n] + \text{noise}[n], \quad n = 1, 2, \dots, N. \end{aligned} \quad (2.1)$$

Here, N is the number of observations used for detection. Once the observations samples are obtained the next step is to evaluate a test statistic $T(\cdot)$, which is basically a function of the observed signal $x[n]$. This test statistic is then compared with a pre-defined or chosen threshold to decide in favor of one of the hypothesis.

$$T(x[1], x[2], \dots, x[N]) \underset{H_0}{\overset{H_1}{\gtrless}} \eta. \quad (2.2)$$

The fundamental design criteria involved in this binary hypothesis problem is (i) how to choose the test statistic and (ii) how to set the detection threshold based on the detection criteria chosen to design the detector. These design criteria depends on different factors such as availability of PU signal knowledge, computational complexity, power constraint, hardware compatibility, performance requirement, and whether the detection of PU is performed by a single SU or multiple SUs are collaborating to detect the availability of PU in the frequency band of interest. In the next section some of the widely used state-of-the-art spectrum sensing techniques are presented.

2.3.1 Techniques

Single user spectrum sensing techniques can be broadly classified into two main categories, viz., coherent techniques and non-coherent techniques. The coherent detection techniques such as the matched filter detector or the cyclostationary feature detector require some prior knowledge about the PU signal. For example, the matched filter detection algorithms make explicit assumptions on the known pilot waveform or the preamble to design the detectors. On the contrary, the non-coherent detection methods do not need any prior information about the PU signal properties or do not make any assumption of PU signal statistics. Fig. 2.2 shows the classification of different spectrum sensing schemes [50]. Here, we present some of the well-known and most used spectrum sensing algorithms. For a more detail list of sensing algorithms please refer to [50, 51].

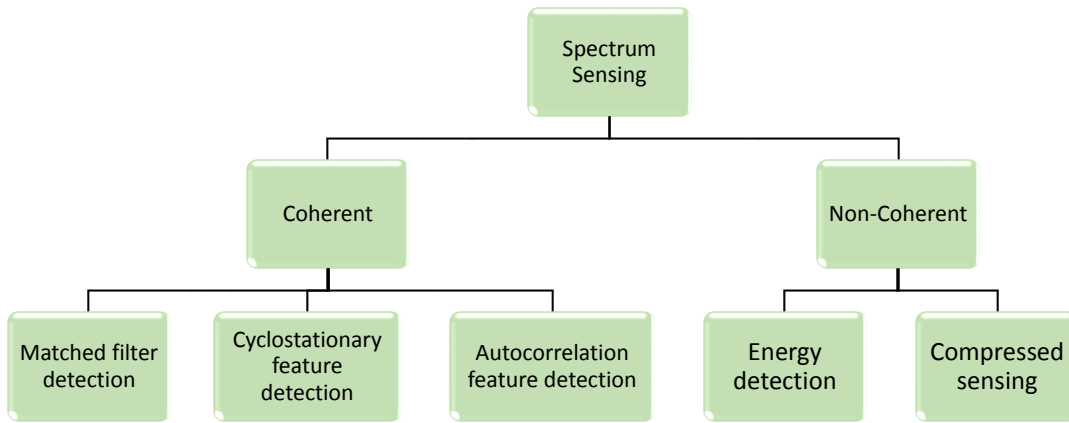


Figure 2.2: Classification of spectrum sensing schemes [50].

- **Matched filter:** When the PU signal information is well known to the CR, the matched filter is the optimal linear filter for maximizing the SNR in the presence of additive white Gaussian noise [24, 52]. In CR framework, the matched filter is obtained by correlating a known signal, or PU signal template, with an unknown signal to detect the presence of PU signal in the unknown signal. This is equivalent to convolving the unknown signal with a time-reversed version of the template.
- **Cyclostationary detection:** In literature, a cyclostationary process is defined as a signal having statistical properties that vary cyclically with time [53]. This feature is present in most of the transmitted communication signals and can be detected and analyzed. Thus, this cyclostationary feature can be used as a means for PU signal detection and recognition. Recent bibliographies on cyclostationarity including a large number of references on cyclostationarity-based detection are provided in [54, 55, 56].
- **Energy Detection:** The classical ED, which is also called the radiometer, measures the received energy and compares it to a threshold. Fig. 2.3 shows the basic block diagram of an ED [57]. In

order to evaluate the energy of the received signal, N number of output samples of the bandpass filter are first taken. These samples are then squared and summed to get the energy value. The ED is an optimal detector when the noise power is perfectly known. In fact, it is one of the most widely used spectrum sensor primarily because of its simplicity, low power consumption, and being non-coherent in nature making it able to detect the presence of any kind of PU signal.

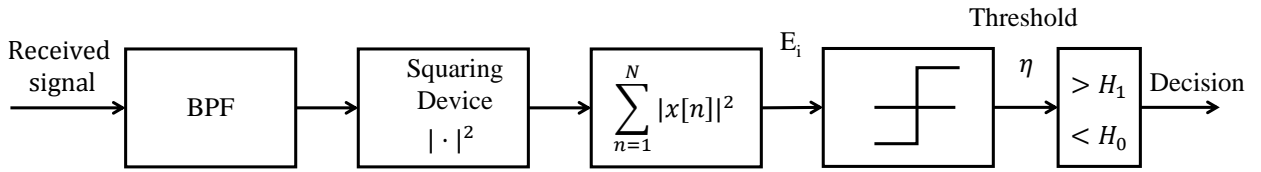


Figure 2.3: Basic block diagram of an ED [57].

2.3.2 Performance criteria

- False alarm probability:** A false alarm is an erroneous target detection decision caused by noise or other interfering signals exceeding the detection threshold. In general, it is an indication of the presence of a target when in reality the target is absent. In the context of CR, false alarm probability (P_{fa}) is defined as the probability that the detector declares the presence of PU, when the PU is actually absent. Consider the binary hypothesis problem in (2.1), as an attempt to distinguish between the hypotheses based on one sample $x[1]$

$$\begin{aligned} H_0 : x[1] &= noise[1] \\ H_1 : x[1] &= signal[1] + noise[1]. \end{aligned} \quad (2.3)$$

If the probability density function (pdf) of $x[1]$ under H_0 is known a priori, then the probability of false alarm for threshold η can be expressed as

$$P_{fa} = \Pr \{x[1] > \eta; H_0\} = \int_{\eta}^{\infty} p(x[1]; H_0) dt. \quad (2.4)$$

In Fig. 2.4, assuming Gaussian distribution under $H_0 \sim \mathcal{N}(\mu_0, \sigma_0^2)$, the shaded portion in blue under $p(x[1]; H_0)$ denotes the false alarm probability. Increase in false alarm rate will lead to higher loss of opportunistic access of spectrum for the SU.

- Missed detection probability:** It is defined as the probability that the detector proclaims the nonattendance of PU, when the PU is actually present. An excessive number of missed detections may lead to collisions of the PU and SU transmissions causing interference to the PU. Therefore, controlling the missed detection probability is crucial for keeping the interference to the PU under

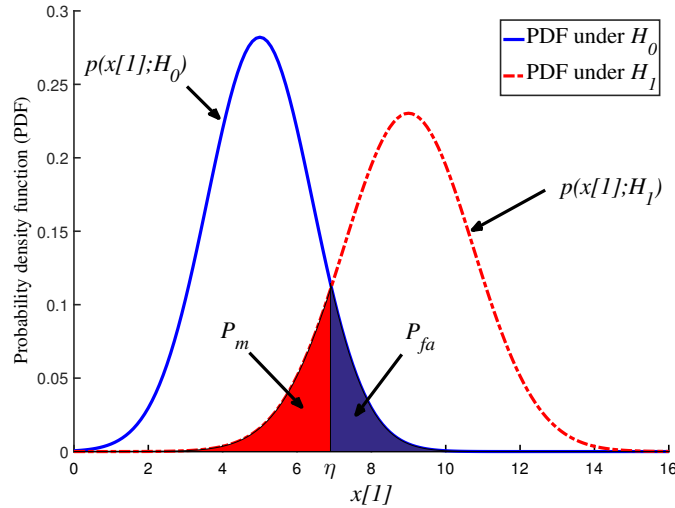


Figure 2.4: Figure showing probability of false alarm (P_{fa}) and probability of miss detection (P_m) with threshold η .

the permissible limits. The probability of missed detection (P_m) can also be expressed in terms of probability of detection (P_d) as

$$P_m = 1 - P_d.$$

Analogous to P_{fa} , if the pdf under hypothesis H_1 is known a priori, P_m can be expressed as

$$P_m = Pr \{x[1] < \eta; H_1\} = \int_{-\infty}^{\eta} p(x[1]; H_1) dt. \quad (2.5)$$

Similarly, from Fig. 2.4, assuming Gaussian distribution under $H_1 \sim \mathcal{N}(\mu_1, \sigma_1^2)$, the shaded portion in red under $p(x[1]; H_1)$ denotes the missed detection probability. The corresponding probability of detection, i.e., P_d can be expressed as

$$\begin{aligned} P_d &= 1 - P_m \\ &= 1 - \int_{-\infty}^{\eta} p(x[1]; H_1) dt \\ &= \int_{\eta}^{\infty} p(x[1]; H_1) dt. \end{aligned} \quad (2.6)$$

- Sensing time:** Sensing time can be defined as the amount of time the detector requires to complete the spectrum sensing process, which starts from collecting observations till reaching at the final decision of whether the PU is present or not. If the receiver chain is time-duplexed for reception and sensing, it is desirable that the sensing durations are shorter and the data transmission durations are longer. If the sensing time is too long, the data transmission duration reduces thereby reducing the throughput of the SUs.

- **SNR:** The SNR at the CR node depends on the transmitted PU signal power and the channel effects of the propagation environment. The knowledge of SNR at the CR also plays a crucial role in determining the detection performance of the detector. It is basically desirable that a detector performs better in low SNR and in many cases a detector is rated based on its ability to detect the PU signal at low SNR regions.
- **Complexity and implementation issues:** All spectrum sensing algorithms that has been proposed in literature, do not have the same complexity and efficiency. It is attractive to have straightforward and implementable detecting algorithms, which are likewise less power hungry. Hence, evaluating the equipment cost and energy efficiency of the sensing scheme is additionally important. For example, cyclostationary based detectors perform much better compared to EDs both in the presence as well as in the absence of NU. However, cyclostationary detectors are more complex and difficult to implement in simple hardware. Moreover, they are computation intensive, hence consume more power to perform the required task. On the contrary, EDs are very simple to implement in any hardware and on top of that they consume very less power to operate.
- **Detecting different PU waveforms:** PU signal can have different waveforms depending on the modulation schemes being deployed in the transmitter section. Capacity to distinguish diverse PU waveforms is an alluring property that an ideal signal detector should possess. However, it may not be possible for all detectors to have this ability to detect all PU waveforms. Some detectors are specifically designed only for a particular PU waveform if we are only interested in that genre of PUs. In this regard, an ED requires special preference because it possesses the ability to detect all kinds of PU signal. However, it cannot distinguish between different waveforms.
- **Robustness against non-idealities:** Non-idealities may arise due to different reasons such as hardware issues, synchronizations problems between transmitter and the receiver, incorrect parameter model assumption etc. Under such circumstances the received signal may lose its originality apart from being already distorted due to channel effects. This may degrade the detector performance more than expected.

2.3.3 Detection criteria

There are several detection criterion available in literature [58, 59, 60]. Some of them are discussed below

- **Bayesian formulation:** in a Bayesian approach, two assumptions are made. First, the a priori probabilities of occurrence of hypotheses H_0 and H_1 are known. The second presumption is that a cost is assigned to each possible decision. The cost is due to the fact that some action will be taken based on a decision made. Finally, the impact of the prior probabilities are taken into account and the detection threshold is chosen to minimize a convex combination of the false-alarm and signal detection probabilities. It is a well-established fact that the likelihood ratio (LR)

is the optimal test statistic for any detection problem. For the binary hypothesis testing problem in (2.3), given the prior probabilities $\pi_0 = \Pr(H_0)$ and $\pi_1 = \Pr(H_1)$ for hypotheses H_0 and H_1 respectively, the Bayes detector makes a decision based on comparing the optimal statistic to a threshold:

$$\mathcal{L}(\mathbf{x}) = \frac{p(\mathbf{x}; H_1)}{p(\mathbf{x}; H_0)} \underset{H_0}{\overset{H_1}{\gtrless}} \frac{\pi_0}{\pi_1},$$

where $\mathcal{L}(\mathbf{x})$ denotes likelihood-ratio, $p(\mathbf{x}; H_0)$ and $p(\mathbf{x}; H_1)$ are pdfs under hypothesis H_0 and H_1 respectively. Furthermore, the optimal detector minimizes the Bayesian error probability

$$P_e = \pi_0 P_{fa} + \pi_1 P_m,$$

or more generally, the detector minimizes the Bayes' risk.

- **Neyman-Pearson formulation:** The most mainstream approach for spectrum sensing in the literature is to utilize the Neyman-Pearson (NP) criterion. This setup is considered when the prior probabilities are unavailable. In NP setting, the objective is to maximize the probability of detection P_d , subject to a constraint on the probability of false alarm, P_{fa} . Analogous to Bayes formulation, in the NP setup also the likelihood ratio (LR) is the optimal test statistic.

$$\mathcal{L}(\mathbf{x}) = \frac{p(\mathbf{x}; H_1)}{p(\mathbf{x}; H_0)} \underset{H_0}{\overset{H_1}{\gtrless}} \eta,$$

while the threshold η is evaluated for a given value of $P_{fa} = \beta$ as

$$P_{fa} = \int_{\{\mathbf{x}: \mathcal{L}(\mathbf{x}) > \eta\}} p(\mathbf{x}; H_0) = \beta. \quad (2.7)$$

- **Minimax criterion:** In many circumstances, we might not have enough data about the prior probabilities and as such, the Bayes' criterion can't be utilized. In such situations we may go for minimax criterion. The fundamental principle of minimax criterion is to select a value P_1 as the priori probability of H_1 for which the risk is maximum, and then minimize that risk function. In other words, this formulation involves minimizing the maximum average cost for the selected prior probability P_1 .
- **Sequential detection:** In this formulation, observations are taken in sequential fashion such that the test is conducted after each observation. Each time an observation is taken, one of the three possible decisions is made - (i) H_0 is true (ii) H_1 is true (iii) Insufficient information to take decision either in favor of H_0 or H_1 . On the off chance that choices (i) or (ii) are made, the hypothesis testing strategy stops. Otherwise, an extra observation is taken, and the test is performed once more. This procedure proceeds until the point when a choice is made either for H_1 or H_0 . Note that the number of observation K is not fixed, but is a random variable. Such a test that makes one of the three possible decisions mentioned above after the k th observation is referred to as sequential likelihood ratio test.

2.4 Cooperative spectrum sensing

In the CR literature, several single CR based spectrum sensing schemes have been described such as energy detection, cyclostationary feature based detection, autocorrelation based detection, eigen-value based detection, etc [51, 50]. However, a single CR device performing spectrum sensing may suffer from multi-path fading, low signal power, shadowing and receiver uncertainty issues. These factors may severely deteriorate the detection performance of the CR [61], which will ultimately hamper its QoS. In order to mitigate the influence of these issues, cooperative spectrum sensing (CSS) schemes have been proposed to enhance detection performance by exploiting spatial diversity [61, 62]. In CSS, a group of CRs or SUs will collaborate to detect the presence or absence of the PU. The added advantage of CSS is that it also increases SNR gain. Furthermore, due to cooperation gain, CR devices based on simple sensing algorithms can be employed instead of complex and power consuming schemes, thus lowering the cost of CR sensor.

2.4.1 Classification and framework of CSS

In CSS literature, it has been broadly classified into three categories: centralized [63, 64], distributed [65] and relay assisted [66, 67]:

- **Centralized:** In the centralized CSS approach, a group of SUs first sense the spectrum via the listening channel. Based on their observations the SUs calculate the sensing information. Next, each SU transmits its sensing data to a central entity called the fusion center (FC) via the reporting channel. The FC applies suitable combination rules on the received data from all the SUs and arrives at a global decision depending on the decision criterion employed at the FC. This global decision is then relayed back to all the SUs. Finally, based on the received information, the SUs adjust their operating parameters accordingly.
- **Distributed:** In this approach, the SUs do not send any sensing data to a FC for decision making. The SUs communicate among themselves iteratively and finally converge to a common decision regarding the status of the frequency, i.e., whether it is occupied or empty.
- **Relay assisted:** Owing to the fact that the listening and reporting channels are imperfect, in this CSS scheme, a CR experiencing a strong listening channel but a weak reporting channel is assisted by another CR to relay the former CR's sensing information to the FC. The sensing data may require multiple hops to reach the destination. Compared to this the centralized and distributed CSS structures are single hop schemes.

In this thesis, centralized structure is considered for CED. Fig. 2.5 shows the framework for this approach. This model is also referred as parallel distributed fusion model [68]. As already described earlier, it consists of a group of spatially distributed CR based SUs observing the spectrum for the presence of the PU through their observations $x_i[n]$. The observed data or sensing information is send

to a FC. The FC combines this reported data using suitable fusion rules and arrives at the global decision. The FC reports back its decision to all the SUs via the reporting channel. In this model all the SUs are assumed to be in sync with the FC in terms of sensing the PU or the frequency band utilized for listening and reporting/control channels.

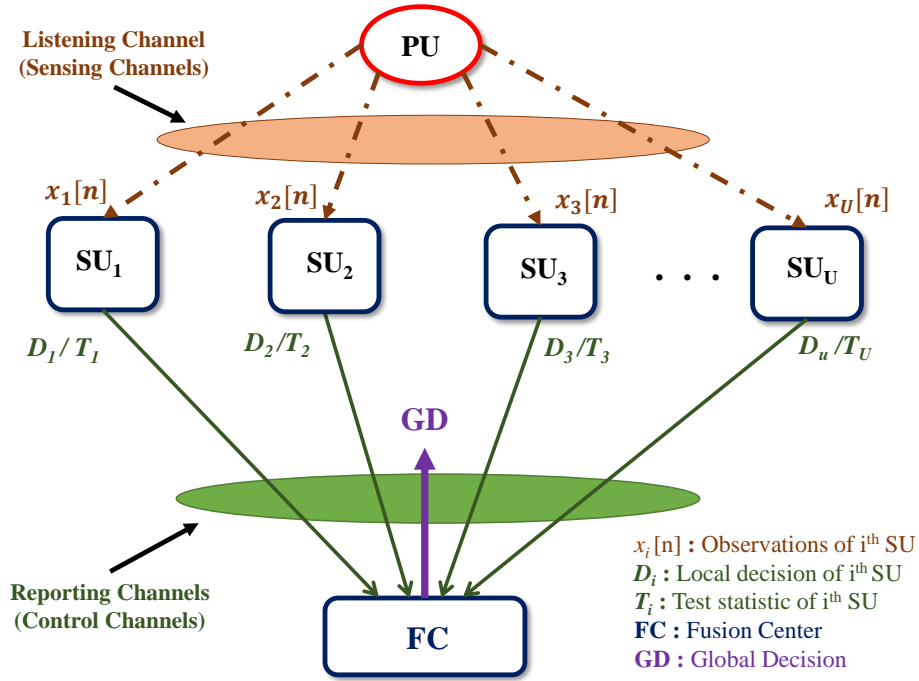


Figure 2.5: Framework for centralized CSS structure. For hard decision combining each SU sends its one bit local decision D_i to the FC. In the soft combining approach, the SUs send their corresponding test statistic, T_i to the FC. The FC reports back the global decision to all the SUs.

The centralized CSS structure can be further classified into two classes: hard decision combining and soft combining depending on the type of sensing data sent to the FC. These schemes are discussed below.

2.4.2 Hard decision combining

In hard decision combining, each of the SUs sends a one-bit hard decision to the FC which fuses these decisions to arrive at the final decision. Examples of one-bit hard decision combining are Boolean fusion rules such as OR, AND, and MAJORITY. Advantages of hard decision combining are that they are easy to implement and reduce the bandwidth requirement on the reporting channel between the sensors and the FC. However, these advantages come at the cost of performance loss resulting from the quantization. Hard decision combining has been well studied in the detection literature [69, 70].

2.4.3 Soft combining

For soft combining based cooperative sensing, each SU sends a quantized version of a local decision statistic such as the log-likelihood ratio or any suitable sufficient statistic to the FC. At the FC, the test statistics from all the SUs are combined using some combination rule which results in a single test statistic. The distribution of this combined test statistic is evaluated beforehand to determine the threshold based on the detection criteria. The global decision is made by comparing the combined test statistic with the pre-fined threshold. It has been shown in [71] that there is considerable performance gain in using soft decisions for cooperative detection as compared to hard decisions for different listening channel conditions and even in the presence of reporting channel errors.

Chapter 3

Sum Fusion Rule based CED and Generalized SNR Wall

Energy detection is the simplest spectrum sensing algorithm among all other sensing schemes. However, it is not robust due to presence of model irregularities. This leads to performance limitations such as formation of SNR wall in the absence of accurate knowledge of noise variance. Moreover, as mentioned in the previous chapter, single user spectrum sensing suffers from path loss, multi-path fading and shadowing effects. This channel imperfections reduces the ED's sensing capability to detect and leads to performance degradation. To dilute the drawbacks of single user detection, cooperative sensing methods were proposed. Cooperation helps in improving detection performance of the entire CR network as it provides diversity gain and SNR gain. In this regard, if all the SUs employ EDs for sensing the spectrum, we refer this collaborative spectrum sensing scheme as CED.

In this chapter, we first discuss the ideal sum fusion rule based CED and its performance in detail assuming complete knowledge of noise distribution parameters. This is a simple and effective soft combining technique, where the final test statistic is the sum of energy values from all the SUs in the CR network. The distribution of this final test statistic is easily computable under conditional independence. Next, the concept of NU in energy detection is brought forward and the various ways of modeling noise variance under NU are presented. Then we again go back to the sum fusion rule based CED, but in the presence of NU. The performance of the CED model under NU varies with the noise variance model used. This point is highlighted in detail in the upcoming sections. Finally, the concept of SNR wall is presented. SNR wall phenomenon is one of the most important and fundamental problem concerning EDs under NU. SNR walls are fundamental limits imposed on the radiometer as a result of model uncertainties in the form of NU [24]. However, in this thesis, the focus is mainly on SNR walls for sum fusion rule based CED. We derive equations of generalized SNR wall for CED model considering heterogeneous nature of SUs involved in the CR network. Finally, it is shown that all other SNR wall expressions, both for a local ED as well as for CED, can be obtained from the generalized SNR wall expression, which we have termed as signal power wall (SP wall).

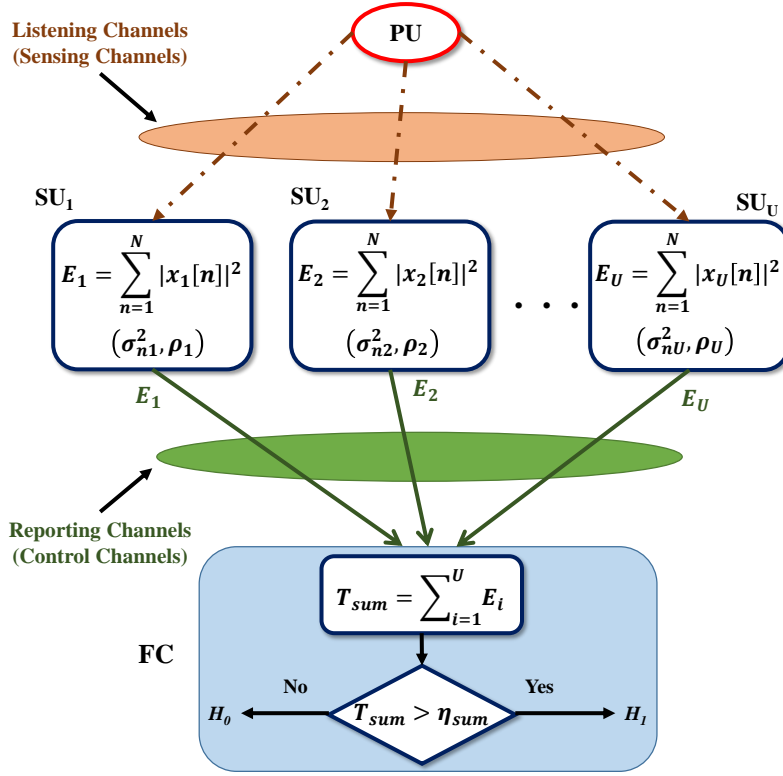


Figure 3.1: Considered CED model: SUs have non-identical NU parameters. Each SU evaluates energy from the observed data and sends it to the FC, where sum fusion rule is applied for decision making.

3.1 System model for sum fusion based CED

The sum fusion rule based CED model with heterogeneous CR nodes is shown in Figure 3.1. It consists of a PU, a fixed number of energy detection based SUs and a FC. Soft combining method is applied, where the SUs send the energy values computed from the observations to the FC. The FC employs sum fusion rule to combine the received data and arrives at the global decision. Moreover, the listening channels are assumed to be additive white Gaussian noise (AWGN) channels while the reporting channels are error-free.

In practical CR networks, it is highly probable that different SUs have different model parameters. Therefore, in this thesis, the participating SUs are considered to be heterogeneous in nature such that the true noise variance σ_i^2 at the i^{th} SU is different for different SUs. This is one of the novel ideas that has been embedded in the CED model. Thus, the concept of heterogeneous SUs in CED makes it more realistic and ultimately paves the path for new results.

Now, if $x_i[n]$ denote the received observations at the i^{th} SU for $n = 1, 2, \dots, N$, then the received signal energy E_i can be evaluated from the N received samples by

$$E_i = \sum_{n=1}^N |x_i[n]|^2. \quad (3.1)$$

Each SU evaluates energy from the observed data and sends it to the FC. At the FC, the sum fusion rule is applied so that the test statistic is given by

$$T_{sum} = \sum_{i=1}^U E_i, \quad (3.2)$$

while the global decision is made by using

$$T_{sum} \underset{H_0}{\overset{H_1}{\gtrless}} \eta_{sum}, \quad (3.3)$$

where η_{sum} is the threshold of a NP detector at the FC. It is assumed that the information about NU parameters of the SUs is available at the FC.

In a distributed detection scheme, the presence or absence of a PU on locally observed signal samples can be formulated as a binary hypothesis testing problem. There are two hypotheses H_0 and H_1 , where H_0 denotes the absence of PU signal and H_1 denotes the presence of PU signal. The considered signal model is

$$\begin{aligned} H_0 : x_i[n] &= w_i[n] \\ H_1 : x_i[n] &= s[n] + w_i[n] \end{aligned} \quad (3.4)$$

for $n = 1, 2, \dots, N$, where $x_i[n]$ and $w_i[n]$, are samples of the received signal and noise respectively at the i^{th} SU while $s[n]$ is the transmitted PU signal sample. The AWGN sample $w_i[n]$ is assumed to be a complex circularly symmetric Gaussian random variable with zero mean and variance σ_i^2 , i.e., $w_i[n] \sim \mathcal{N}_c(0, \sigma_i^2)$. Without loss of generality, $s[n]$ and $w_i[n]$ are assumed to be independent of each other. Moreover, the noise samples $w_i[n]$ are also assumed to be independent from sensor to sensor. Several types of PU waveforms such as OFDM signals are Gaussian signals [7]. Therefore, the PU signal $s[n]$ is also assumed to be a complex circularly symmetric Gaussian random variable with zero mean and variance σ_s^2 . Consequently, $x_i[n]$ is also a complex circularly symmetric Gaussian random variable with zero mean and variance σ_x^2 , i.e., $x_i[n] \sim \mathcal{N}_c(0, \sigma_x^2)$ under the two hypotheses. Therefore, we have

$$\begin{aligned} H_0 &: x_i[n] \sim \mathcal{N}_c(0, \sigma_i^2) \\ H_1 &: x_i[n] \sim \mathcal{N}_c(0, \sigma_s^2 + \sigma_i^2). \end{aligned} \quad (3.5)$$

Since E_i given in (3.1) is the sum of the squares of N complex Gaussian random variables, therefore, $\frac{E_i}{\sigma_i^2/2}$ follows a central chi-square (χ^2) distribution with $2N$ degrees of freedom [72] under H_0 and a non-central χ^2 distribution under H_1 [31] so that

$$\begin{aligned} H_0 &: \frac{2E_i}{\sigma_i^2} \sim \chi_{2N}^2 \\ H_1 &: \frac{2E_i}{\sigma_i^2} \sim \chi_{2N}^2(\lambda_i), \end{aligned} \quad (3.6)$$

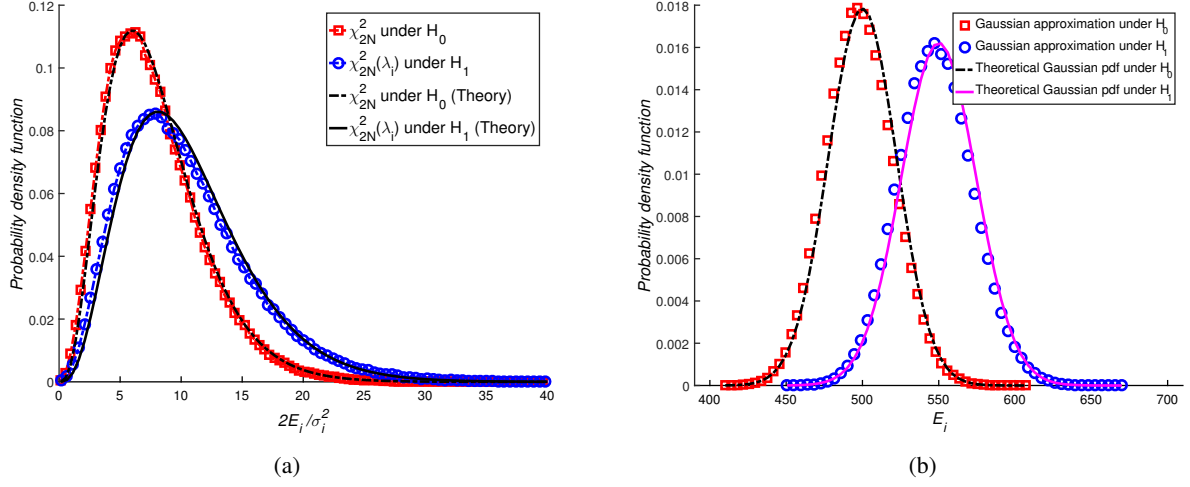


Figure 3.2: (a) Distribution of $2E_i/\sigma_i^2$ for $N = 5$ and $\text{SNR} = -5$ dB. (b) Asymptotic distribution of E_i for $N = 500$ and $\text{SNR} = -10$ dB.

where λ_i is the non-centrality parameter of the i^{th} SU and is given as in [31] as

$$\lambda_i = \frac{\sum_{n=1}^N |s[n]|^2}{\sigma_i^2/2} \quad (3.7)$$

However, according to the central limit theorem [73], if the number of samples N is sufficiently large (e.g., > 100), the test statistic E_i is asymptotically Gaussian distributed, and its distributions at the i^{th} SU under the two hypotheses H_0 and H_1 , are given in [31, 74] as

$$\begin{aligned} H_0 : E_i &\sim \mathcal{N}(\mu_{0i}, \sigma_{0i}^2), \\ H_1 : E_i &\sim \mathcal{N}(\mu_{1i}, \sigma_{1i}^2), \end{aligned} \quad (3.8)$$

where

$$\begin{aligned} \mu_{0i} &= N\sigma_i^2 \quad ; \quad \mu_{1i} = N\sigma_i^2(1 + \text{SNR}_i) = N(\sigma_i^2 + P) \\ \sigma_{0i}^2 &= N\sigma_i^4 \quad ; \quad \sigma_{1i}^2 = N\sigma_i^4(1 + \text{SNR}_i)^2 = N(\sigma_i^2 + P)^2. \end{aligned}$$

Here, $\text{SNR}_i = P/\sigma_i^2$ is the true signal-to-noise-ratio (SNR) at the i^{th} SU with P denoting the transmitted PU average signal power. Corresponding SNR in dB scale is given by $\text{SNR}_i(\text{dB}) = 10 \log_{10} \text{SNR}_i$.

In our work, we have considered NP based detector, where the prime objective is to maximize the P_d (or minimize P_m) for a given P_{fa} . The threshold η_{sum} for a NP detector depends on the distribution of T_{sum} under the null hypothesis H_0 and the constraint on the probability of false alarm $P_{fa} \leq \beta$. As T_{sum} in (3.2) is a linear combination of U independent Gaussian random variables, therefore, it is also Gaussian distributed under both the hypotheses H_0 and H_1 as given in [31] by

$$\begin{aligned} H_0 : T_{sum} &\sim \mathcal{N}(\mu_0, \sigma_0^2), \\ H_1 : T_{sum} &\sim \mathcal{N}(\mu_1, \sigma_1^2), \end{aligned} \quad (3.9)$$

where

$$\begin{aligned}\mu_0 &= N \sum_{i=1}^U \sigma_i^2 \quad ; \quad \mu_1 = N \sum_{i=1}^U (\sigma_i^2 + P) \\ \sigma_0^2 &= N \sum_{i=1}^U \sigma_i^4 \quad ; \quad \sigma_1^2 = N \sum_{i=1}^U (\sigma_i^2 + P)^2.\end{aligned}\tag{3.10}$$

Assuming that the complete knowledge of noise variance σ_i^2 of all the SUs is available, the P_{fa} and the P_d for a NP detector are expressed as given in [72] by

$$P_{fa} = Q\left(\frac{\eta_{sum} - \mu_0}{\sigma_0}\right),\tag{3.11}$$

$$P_d = Q\left(\frac{\eta_{sum} - \mu_1}{\sigma_1}\right),\tag{3.12}$$

where $Q(\cdot)$ is the tail probability of the standard normal distribution. The threshold η_{sum} with false alarm constraint of β can be calculated from (3.11) as given in [72]

$$\begin{aligned}\eta_{sum} &= Q^{-1}(\beta)\sigma_0 + \mu_0 \\ &= Q^{-1}(\beta)\sqrt{N \sum_{i=1}^U \sigma_i^4 + N \sum_{i=1}^U \sigma_i^2},\end{aligned}\tag{3.13}$$

Note that the sum fusion rule given by (3.2) is also an optimal fusion rule for binary hypothesis testing problem in (3.9) when noise variance is perfectly known [31, 72].

3.2 Effect of NU

In most of the cases, it is assumed that the noise variance is exactly known. For perfectly known noise variance case, the detection performance of an ED can be perfectly mapped using analytical models. However, noise variance may fluctuate from time to time and from place to place due to several reasons such as temperature and out of band interference. In addition to that, in practical systems, the noise variance is estimated at the receiver based on a finite number of observed samples in a zero signal band. As a result, the noise variance estimate is bound to have some uncertainty or variability.

The performance of an ED in the presence of NU has been studied in many works. The knowledge of AWGN is crucial for an ED. This is because the threshold for an ED depends on the noise variance. Similarly for CED, the threshold at the FC is a function of noise variance at the individual SU as can be seen in (3.13). Therefore, when there is uncertainty in noise variance estimate, the overall detection performance of CED varies from the ideal case.

3.2.1 NU models

In the following sections we discuss different ways of modeling NU. The first model of noise variance is assuming it to be an unknown constant within some known interval. This approach is basically based

on classical theory of estimation. The second way of modeling the noise variance is assuming it to be a random variable with a known distribution. Both these models are discussed in detail.

1. **Noise as an unknown constant:** In this case, the NU at each SU is modeled as in [24] by considering σ_i^2 to be an unknown constant in the interval $\left(\frac{1}{\rho_i}\sigma_{ni}^2, \rho_i\sigma_{ni}^2\right)$ where σ_{ni}^2 is the nominal noise variance and $\rho_i \geq 1$ is the uncertainty parameter for the i^{th} SU. Nominal SNR corresponding to the nominal noise variance σ_{ni}^2 is denoted as $\text{SNR}_{ni} = P/\sigma_{ni}^2$. Corresponding nominal SNR in dB scale is denoted by $\text{SNR}_{ni}(\text{dB}) = 10 \log_{10} \text{SNR}_{ni}$. As it is sometimes convenient to describe the uncertainty parameter in dB scale, we denote the deviation in noise variance about the nominal value in dB for the i^{th} SU by $\Delta_i = 10 \log_{10} \rho_i$. Therefore, if the deviation of noise variance σ_i^2 about its nominal or average value σ_{ni}^2 is $\pm\Delta_i$ dB then the lower bound σ_{li}^2 and upper bound σ_{ui}^2 on the noise variance are given by

$$\begin{aligned}\sigma_{li}^2 &= \sigma_{ni}^2 \cdot 10^{(-\Delta_i/10)} = \frac{1}{\rho} \sigma_{ni}^2 \\ \sigma_{ui}^2 &= \sigma_{ni}^2 \cdot 10^{(+\Delta_i/10)} = \rho \sigma_{ni}^2.\end{aligned}\tag{3.14}$$

2. **Noise as a random variable:** In the second NU model, we have assumed the noise variance to be a random variable having a known distribution. We consider two widely-used distributions for modeling the noise variance: *Gaussian* and *uniform*. In most of the scenarios, noise variance is not known and has to be estimated. Most of the estimators of noise variance (σ_i^2) for AWGN would result in the estimate to be Gaussian distributed. For example, the asymptotic distribution of the maximum likelihood estimate of σ_i^2 has Gaussian distribution [75]. The probability density function (pdf) of the noise variance σ_i^2 assuming it to be Gaussian distributed is given by

$$f(\sigma_i^2) = \frac{1}{\sqrt{2\pi}\sigma_\Delta} \exp\left(-\frac{(\sigma_i^2 - \sigma_n^2)^2}{2\sigma_\Delta^2}\right),\tag{3.15}$$

where σ_n^2 is the mean value and σ_Δ the standard deviation.

When, the only prior information regarding the noise variance is the limits within which the value lies, in that case, uniform distribution is a natural choice. Note that uniform distribution is the least informative probability model as it does not favor any particular value of noise-variance. The uniform distribution for σ_i^2 is given as

$$f(\sigma_i^2) = \begin{cases} \frac{1}{\sigma_U^2 - \sigma_L^2}, & \sigma_L^2 \leq \sigma_i^2 \leq \sigma_U^2 \\ 0, & \text{otherwise} \end{cases}\tag{3.16}$$

where σ_U^2 and σ_L^2 are the upper and the lower bounds of σ_i^2 under uniform distribution. For convenience of specifying both the distributions given in (3.15) and (3.16) in terms of the same distribution parameters, σ_U^2 and σ_L^2 are chosen in this thesis as

$$\begin{aligned}\sigma_U^2 &= \sigma_n^2 + \sqrt{3}\sigma_\Delta, \\ \sigma_L^2 &= \sigma_n^2 - \sqrt{3}\sigma_\Delta.\end{aligned}\tag{3.17}$$

3.2.2 Sum fusion rule under NU

1. **Performance considering noise variance as an unknown constant:** In the presence of NU, (3.13) cannot be used to determine the threshold of NP detector as σ_i^2 is unknown. In such a scenario, to maintain the constraint on the false alarm probability $P_{fa} \leq \beta$ for all values of noise variance within the known interval $\left(\frac{1}{\rho_i}\sigma_{ni}^2, \rho_i\sigma_{ni}^2\right)$, we can set β to be the worst-case false alarm probability [24] corresponding to σ_{ui}^2 so that

$$\begin{aligned}\beta &= \max_{\sigma_i^2 \in \left[\frac{1}{\rho_i}\sigma_{ni}^2, \rho_i\sigma_{ni}^2\right]} Q\left(\frac{\eta'_{sum} - \mu_0}{\sigma_0}\right) \\ &= Q\left(\frac{\eta'_{sum} - N \sum_{i=1}^U \rho_i \sigma_{ni}^2}{\sqrt{N \sum_{i=1}^U \rho_i^2 \sigma_{ni}^4}}\right),\end{aligned}\quad (3.18)$$

where η'_{sum} denotes the threshold of NP detector at the FC in the presence of NU and can be evaluated from (3.18) as

$$\eta'_{sum} = Q^{-1}(\beta) \sqrt{N \sum_{i=1}^U \rho_i^2 \sigma_{ni}^4 + N \sum_{i=1}^U \rho_i \sigma_{ni}^2}.\quad (3.19)$$

The probability of detection for the worst case scenario is as given in [24]

$$\begin{aligned}P_d &= \min_{\sigma_i^2 \in \left[\frac{1}{\rho_i}\sigma_{ni}^2, \rho_i\sigma_{ni}^2\right]} Q\left(\frac{\eta'_{sum} - \mu_1}{\sigma_1}\right) \\ &= Q\left(\frac{\eta'_{sum} - N \sum_{i=1}^U \left(\frac{1}{\rho_i}\sigma_{ni}^2 + P\right)}{\sqrt{N \sum_{i=1}^U \left(\frac{1}{\rho_i}\sigma_{ni}^2 + P\right)^2}}\right).\end{aligned}\quad (3.20)$$

2. **Performance considering noise variance as random variable:** Under the random variable assumption of σ_i^2 , the P_{fa} and P_d at FC cannot be expressed using (3.11) and (3.12) respectively. In this case, we need to evaluate the average probability of false alarm (P'_{fa}) and average probability of detection (P'_d) at the FC, which are given by

$$P'_{fa}(\bar{\eta}_{sum}, \sigma_\Delta^2) = \int_0^\infty Q\left(\frac{\bar{\eta}_{sum} - \mu_0}{\sigma_0}\right) f(\sigma_i^2) d\sigma_i^2,\quad (3.21)$$

$$P'_d(\bar{\eta}_{sum}, \sigma_\Delta^2) = \int_0^\infty Q\left(\frac{\bar{\eta}_{sum} - \mu_1}{\sigma_1}\right) f(\sigma_i^2) d\sigma_i^2.\quad (3.22)$$

Therefore, under this noise variance model, the threshold $\bar{\eta}_{sum}$ at the FC is determined using equation (3.21) for a desirable probability of false alarm. Moreover, we can see that the two

average probabilities, i.e., P'_{fa} and P'_d are functions of only the distribution parameter σ_Δ^2 as the noise variance σ_w^2 is integrated out. Furthermore, in this case, we define average signal-to-noise ratio as, $ASNR = \sigma_s^2/\sigma_n^2$. In dB scale, ASNR is expressed as, $ASNR \text{ (dB)} = 10\log_{10}(\sigma_s^2/\sigma_n^2)$.

3.3 SNR wall

In an ED, the actual performance can deviate significantly from the prediction in the presence of NU. In the presence of NU, ED suffers from a performance limitation such that if the nominal SNR at the SU is below a certain SNR threshold, it fails to achieve the desired P_d and P_{fa} even if the number of samples N tends to infinity. The nominal SNR threshold below which this phenomenon occurs is called the *SNR wall* for the detector. The existence of SNR wall for a local ED was first shown in [24] where the noise was modeled as an unknown constant within an interval determined by its uncertainty parameters. SNR wall for CSS was proposed in [25, 26]. However, the papers in CED literature have derived the SNR wall for homogeneous case when all the SUs have same nominal noise-variances and same uncertainty-intervals. In our work, we derive the SNR wall for a more general case of heterogeneous SUs, where each SU may have different noise variance as well as different uncertainty interval.

3.4 Generalized SNR wall

In this section, we first derive the generalized SNR wall expressions for CED under the general assumption that all the participating CR nodes or SUs are heterogeneous in nature. Later, it is shown that the traditional SNR wall expressions for local as well as CED with homogeneous sensors can be obtained as special cases of the generalized SNR wall expression.

In the current CED model, under NU, with noise variance being modeled as an unknown constant, the expressions for threshold η'_{sum} and probability of detection P_d for false alarm constraint of β are given as

$$\eta'_{sum} = Q^{-1}(\beta) \sqrt{N \sum_{i=1}^U \rho_i^2 \sigma_{ni}^4 + N \sum_{i=1}^U \rho_i \sigma_{ni}^2} \quad (3.23)$$

$$\begin{aligned} P_d &= \min_{\sigma_i^2 \in \left[\frac{1}{\rho_i} \sigma_{ni}^2, \rho_i \sigma_{ni}^2 \right]} Q \left(\frac{\eta'_{sum} - \mu_1}{\sigma_1} \right) \\ &= Q \left(\frac{\eta'_{sum} - N \sum_{i=1}^U \left(\frac{1}{\rho_i} \sigma_{ni}^2 + P \right)}{\sqrt{N \sum_{i=1}^U \left(\frac{1}{\rho_i} \sigma_{ni}^2 + P \right)^2}} \right). \end{aligned} \quad (3.24)$$

Now substituting (3.23) in (3.24), we get the expression for the sample size N as

$$N = \frac{\left[Q^{-1}(P_{fa}) \sqrt{\sum_{i=1}^U \rho_i^2 \sigma_{ni}^4} - Q^{-1}(P_d) \sqrt{\sum_{i=1}^U \left(\frac{1}{\rho_i} \sigma_{ni}^2 + P \right)^2} \right]^2}{\left[\sum_{i=1}^U \left(\frac{1}{\rho_i} \sigma_{ni}^2 + P \right) - \sum_{i=1}^U \rho_i \sigma_{ni}^2 \right]^2}. \quad (3.25)$$

For the considered case, $N \rightarrow \infty$ as the denominator in (3.25) approaches zero. Therefore, to derive the generalized SNR wall for the considered scenario, equating the denominator of (3.25) to zero and simplifying it further, we get

$$P^* = \frac{1}{U} \sum_{i=1}^U \sigma_{ni}^2 \left(\rho_i - \frac{1}{\rho_i} \right). \quad (3.26)$$

From (3.26), we can clearly observe that in the case of SUs having heterogeneous nominal noise variances σ_{ni}^2 , defining a single SNR wall for all the SU is not feasible since each SU will have its own nominal SNR values for the same average signal power P^* . Therefore, instead of defining a SNR wall for each SU, we take the average signal power as the reference, to coin a new term called *signal power (SP) wall* denoted by SP_{wall} , which is given as

$$\boxed{\text{SP}_{\text{wall}} = P^* = \frac{1}{U} \sum_{i=1}^U \sigma_{ni}^2 \left(\rho_i - \frac{1}{\rho_i} \right)}. \quad (3.27)$$

The above equation signifies that for a CR network performing CED consisting of CR nodes with heterogeneous NU parameters (heterogeneous both in nominal noise variance and uncertainty factor), the minimum average signal power, P_{\min} , required to achieve the target P_d and P_{fa} at the FC should always be greater than SP_{wall} , i.e. $P_{\min} > \text{SP}_{\text{wall}}$.

3.4.1 SNR wall as a special case of SP wall

For $\sigma_{ni}^2 = \sigma_n^2$, (3.27) can be written as

$$\text{SP}_{\text{wall}} = \frac{\sigma_n^2}{U} \sum_{i=1}^U \left(\rho_i - \frac{1}{\rho_i} \right). \quad (3.28)$$

Using $\text{SNR} = P/\sigma_n^2$, we can rewrite the above equation as

$$\text{SNR}_{\text{wall}} = \frac{\text{SP}_{\text{wall}}}{\sigma_n^2} = \frac{1}{U} \sum_{i=1}^U \left(\rho_i - \frac{1}{\rho_i} \right). \quad (3.29)$$

For homogeneous CR nodes, where $\rho_i = \rho$ in addition to $\sigma_{ni}^2 = \sigma_n^2$, we can rewrite (3.29) as

$$\text{SNR}_{\text{wall}} = \frac{\text{SP}_{\text{wall}}}{\sigma_n^2} = \left(\rho - \frac{1}{\rho} \right). \quad (3.30)$$

This is the expression for traditional SNR wall as shown in [24] for local ED and in [25, 26] for CED. From this we can conclude that CED using traditional soft combining fusion rule does not contribute in lowering the SNR wall. However, when $\text{SNR}_n > \text{SNR}_{\text{wall}}$, cooperation does help in reducing the sample size N at individual SU for achieving the same detection performance. This can be seen from the following expression

$$N = \frac{[\rho Q^{-1}(P_{fa}) - (1/\rho + \text{SNR}_n)Q^{-1}(P_d)]^2}{U [(1/\rho + \text{SNR}_n) - \rho]^2}, \quad (3.31)$$

which can be obtained by using $\rho_i = \rho$ and $\sigma_{ni}^2 = \sigma_n^2$ in (3.25). From (3.31), it is observed that for homogeneous CED case under the condition when $\text{SNR}_n > \text{SNR}_{\text{wall}}$, the sample size N is inversely proportional to the number of CR sensors, i.e., U .

3.5 SP wall analysis and comparison in sum rule based CED

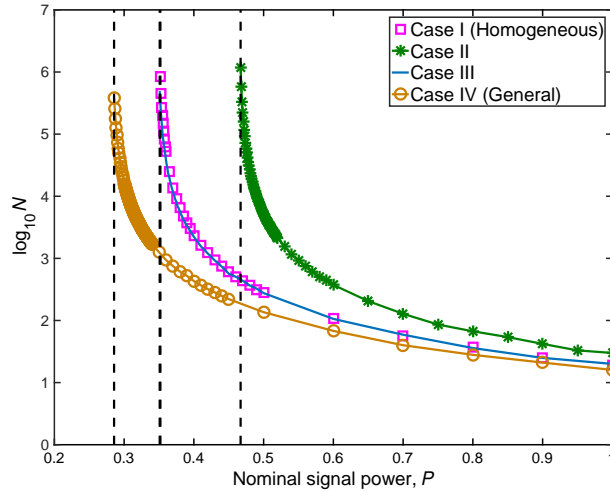
In order to verify the formation of SP wall in the sum rule based CED under NU, four different cases are taken into account based on different combination of nominal noise variance σ_{ni}^2 and uncertainty factor ρ_i . They are as follows:

- Case I: All SUs have identical nominal noise variances and uncertainty parameters (homogeneous).
- Case II: All SUs have different nominal noise variance but identical uncertainty factor.
- Case III: All SUs have identical nominal noise variance but different uncertainty factor.
- Case IV: All SUs have different nominal noise variance and uncertainty factor (the most general scenario).

Table 3.1 shows the four scenarios considered for NU parameters consisting of the nominal noise variances σ_{ni}^2 of the SUs, the deviation Δ_i associated with each SU and its corresponding uncertainty factor ρ_i . For generalized SNR wall, the constraint on the probabilities of detection and false alarm are $P_d \geq 0.9$ and $P_{fa} \leq \beta = 0.1$, respectively.

Table 3.1: The considered heterogeneous cases of NU.

Case	NU parameters ($U = 3$)
I	$\sigma_{n1}^2 = \sigma_{n2}^2 = \sigma_{n3}^2 = 1$ $\Delta_1 = \Delta_2 = \Delta_3 = 0.75$ dB $\rho_1 = \rho_2 = \rho_3 = 1.189$
II	$\sigma_{n1}^2 = 0.9, \sigma_{n2}^2 = 1, \sigma_{n3}^2 = 1.1$ $\Delta_1 = \Delta_2 = \Delta_3 = 1$ dB $\rho_1 = \rho_2 = \rho_3 = 1.259$
III	$\sigma_{n1}^2 = \sigma_{n2}^2 = \sigma_{n3}^2 = 1$ $\Delta_1 = 0.5, \Delta_2 = 0.75, \Delta_3 = 1$ dB $\rho_1 = 1.122, \rho_2 = 1.188, \rho_3 = 1.259$
IV	$\sigma_{n1}^2 = 0.9, \sigma_{n2}^2 = 1, \sigma_{n3}^2 = 1.1$ $\Delta_1 = 0.25, \Delta_2 = 0.5, \Delta_3 = 1$ dB $\rho_1 = 1.0593, \rho_2 = 1.122, \rho_3 = 1.259$


 Figure 3.3: Sample size N (in log scale) vs average signal power, P for case I, II, III and IV.

For simulating the SP wall phenomena for the sum fusion rule based CED, we take 3 SUs in the CR network. For each case the NU parameters are adjusted according to the parameters mentioned in table 3.1. The simulations start with low values of sample size N while the average power P begins with a high value of 1. As we keep decreasing the value of P , the sample size starts increasing in order to achieve the required detection performance of $P_{fa} = 0.1$ and $P_d = 0.9$. Finally, at a particular value of P (depending on the case involved), the sample size grows too large $\approx 10^6$. At this stage the simulation is terminated and the final N value is noted. Fig. 3.3 shows the plots of sample size N (in log scale) vs average PU signal power for all the four cases. The figure clearly demonstrates the existence of SP wall

Table 3.2: SP wall: theory vs simulated.

Case No.	I	II	III	IV
SP _{wall} (Theory)	0.349	0.4646	0.3475	0.2818
SP _{wall} (Simulated)	0.3520	0.4670	0.3510	0.2846

for all the scenarios, heterogeneous (case II, III and IV) as well homogeneous (case I). Table 3.2 shows comparison of theoretical and simulated SP wall values for the sum fusion rule, where the theoretical values of SP wall for all the four cases are calculated using (3.27). It can be seen that both the theoretical and simulated values of SP wall are very close, which validates the theoretical analysis.

Chapter 4

Dempster-Shafer Theory of Evidence

The DST of evidence or in short evidence theory was introduced by Arthur. P. Dempster in the late 1970s in a series of seminal work [76, 77, 78] as a way of representing epistemic¹ knowledge. This theory was later developed by his student Glenn Shafer in [27] as an alternative to the probability theory to fulfill the need of dealing with both imprecision and uncertainty in the observed data. However, in order to appreciate the need of evidence theory as an alternative to probability theory, it is important to understand the limitation of probability theory.

Before the advent of DST, probability or Bayesian theory has been the most widely used theory to deal with imperfect information and uncertain data. The measure of probability expresses the degree of confidence that someone assigns to the occurrence of a realization of an event. If $\Theta = \{\theta_1, \theta_2, \dots, \theta_n\}$ denotes the set of possible mutually exclusive and exhaustive realizations or hypotheses, then probability theory assigns precise probability numbers to each member of Θ . In reality, such assignment is hardly possible since no one knows the chances of occurrence of an event with 100% accuracy. Probability theory enables fusion of information coming from various sources by using the expression of total probability.

$$\Pr(A) = \sum_{i=1}^s \Pr(A|\text{source}_i)\Pr(\text{source}_i),$$

where A is the event under consideration. When the prior probabilities are unknown or there is no reliable information about them, probability theory assigns equal probability to all elements of Θ . This is the way to model ignorance in probability theory. This theory can also deal with imprecision, but the probability of an imprecise event is strongly dependent on the probabilities of precise events. In a lot of cases, the prior information is not available and the user does not have all the data to solve the problem. Moreover, imperfect information, especially the imprecise one, is hardly modeled with the probability theory. Here, we chose evidence theory to deal with uncertainty present in the CED model and develop a novel scheme to improve its performance.

¹Analogues to epistemology, which studies the nature of knowledge, justification, and the rationality of belief.

4.1 Frame of discernment

In order to apply the evidence theory to a particular problem, we need to first define a set of mutually exclusive and exhaustive possible states or hypotheses that the event under observation can take. This initial set of hypotheses is called *Frame of Discernment* from which we obtain all other feasible outcomes of the event. Let us define a frame of discernment say $\Theta = \{\theta_1, \theta_2, \theta_3\}$, where θ_1, θ_2 and θ_3 are the only mutually exclusive and exhaustive hypotheses of the event under observation. Here, mutually exclusive signifies that at most one has to be true, while mutually exhaustive means that at least one θ_i has to be true. Next, the power set of Θ is denoted as $2^\Theta = \{\phi, \theta_1, \theta_2, \theta_3, \{\theta_1, \theta_2\}, \{\theta_1, \theta_3\}, \{\theta_2, \theta_3\}, \Theta\}$ and it represents all the subsets of Θ . Generally, Bayesian theory is more concerned with evidence that supported single conclusions, e.g., evidence for each outcome θ_i in Θ . On the other hand DST is concerned with evidences which support singletons as well as subsets of outcomes in Θ , e.g., $\{\theta_1, \theta_2\}$, $\{\theta_2, \theta_3\}$, etc.

4.2 Basic mass assignment

Once the frame of discernment is fixed and the power set is obtained, the next step for an observer is to assign some weight or belief mass to the various elements of power set 2^Θ . This is the key difference between the DST and the Bayesian theory where instead of assigning belief mass just to the elements of Θ , DST assigns mass to the elements of 2^Θ . This is accomplished by mapping each and every element of 2^Θ to some value between 0 and 1.

DEFINITION: If Θ is a frame of discernment, then a function $m : 2^\Theta \rightarrow [0, 1]$ is called a *basic mass assignment* whenever [27]

1. $m(\phi) = 0$
2. $\sum_{A \subseteq \Theta} m(A) = 1$

The basic mass $m(A)$ of a given member of the power set 2^Θ expresses the proportion of all relevant and available evidence that supports the claim that the actual state belongs to A but to no particular subset of A . For example if $m(A, B) = 0.4$, it means that there is evidence for $\{A, B\}$ as a whole that cannot be divided among more specific beliefs for A and B . The value of $m(A)$ always obeys $0 \leq m(A) \leq 1$. Here it is assumed that $m(\phi) = 0$, which means that at least one of the hypothesis has to be true. However, for this property to hold, the frame of discernment Θ , should be complete and it must contain all possible hypotheses of the scenario considered. Next, (2) signifies that all statements of a single data source have to be normalized, to ensure that the evidence presented by each data source is equal in weight.

In DST, some publications refer m as *basic probability assignment* [27], some call it *basic belief assignment* [79] or the *mass assignment function*. However, in this work, m is denoted as basic mass assignment (BMA) since using basic probability assignment (BPA) may be confusing and misleading

since these are not exactly probability values. There are few more significant points that differentiate the DST from the Bayesian theory. In evidence theory the following axioms are not mandatory

- $m(\Theta) = 1$
- $m(A) \leq m(B)$ if $A \subset B$
- There should be any relationship between $m(A)$ and $m(A^c)$.

Example: Consider the following proposition: *Life on other planet?* Suppose we are asked to assign weights for the proposition “Is there any life on other planet?”. Some scientist may have evidence on this question but most of us will profess complete ignorance about it. Let us define the frame of discernment in this case by $\Theta = \{\theta_0, \theta_1\}$, where θ_0 stands for the hypothesis that there is no life on other planet and θ_1 stands for the hypothesis that life strives on other planet. From the Bayesian theory, we may assign weights as $\{0.5, 0.5\}$, which basically accounts for the least informative scenario when our knowledge is null or minimal. However, in DST, based on the available evidence at our disposal, we can assign weights to all four possibilities $\{\phi, \theta_0, \theta_1, \{\theta_0, \theta_1\}\}$ as $\{0, 0.1, 0.2, 0.7\}$ say. Here, $\{\theta_0, \theta_1\} = 0.7$ signifies our inability to decide or lack of knowledge or ignorance level or amount of uncertainty or how much we don’t know. In fact, if our evidence is null we can assign weights as $\{0, 0, 0, 1\}$, with $\{\theta_0, \theta_1\} = 1$, which basically means that our ignorance level is 100%. This grants DS theory more flexibility and allows for the inclusion of unquantified uncertainty.

From the above example, we observe that the Bayesian theory cannot deal so readily with the representation of ignorance. The basic difficulty is that the theory cannot distinguish between lack of belief and disbelief. It does not allow one to withhold belief from a proposition without according that belief to the negation of the proposition. Summarizing the above example, we can say that in classical Bayesian philosophy if the probability that an event will occur is p , then the probability q , that the event will not occur is given as $q = 1 - p$, irrespective of the fact that we may have no prior knowledge or information on the probability of event not occurring. In evidence theory the author has given us an alternative way of assigning measure of belief or degree of support to a particular fact or event. It is not mandatory to assign a degree of support to a particular fact/event if we do not have substantial evidence at our disposal. Thus, assigning a support value of p to an event say A , does not imply that support for its complement \bar{A} is $1 - p$. We can assign 0 to \bar{A} if we do not have any evidence to support its claim. Hence evidence theory is founded on appending a third category “don’t know” to the familiar dichotomy “it’s true” or “it’s false”. In other words, a DS model provides three non-negative probabilities (p, q, r) with $p + q + r = 1$ to the three categories of the modal triad “known to be true”, “known to be false”, and “don’t know” associated with each assertion specified in the model. Therefore, p signifies our evidence “for the truth” of an assertion, q denote evidence “against” and $r = 1 - p - q$ quantifies residual ambiguity [29, 80]. In the upcoming subsections, we shall go through the other definitions and axioms of evidence theory.

4.3 Belief functions

DEFINITION (a): Suppose Θ is a finite set, and let 2^Θ denote all the subsets of Θ then the function $\text{Bel} : 2^\Theta \rightarrow [0, 1]$ is called a *belief function* over θ if and only if it satisfies all the following conditions [27]:

1. $\text{Bel}(\phi) = 0$.
2. $\text{Bel}(\Theta) = 1$.
3. For every positive integer n and every collection A_1, \dots, A_n of subsets of Θ ,

$$\begin{aligned} \text{Bel}(A_1 \cup \dots \cup A_n) &\geq \sum_i \text{Bel}(A_i) - \sum_{i < j} \text{Bel}(A_i \cap A_j) + \dots + (-1)^{n+1} \text{Bel}(A_1 \cap \dots \cap A_n) \\ &\geq \sum_{\substack{I \subseteq \{1, \dots, n\} \\ I \neq \phi}} (-1)^{|I|+1} \text{Bel} \left(\bigcap_{i \in I} A_i \right), \end{aligned}$$

Such a probability arises when the set Θ is interpreted as a set of possibilities where exactly one of them corresponds to the truth. For each subset A of Θ , the number $\text{Bel}(A)$ can then be interpreted as one's degree of belief that the truth lies in A , and the above mentioned rules (1)-(3) can be understood as rules governing this degree of belief.

The quantity $m(A)$ measures the belief that one commits exactly to A , but not the total belief that one assigns to A . To obtain the measure of the total belief committed to A , one must add to $m(A)$ the quantities $m(B)$ for all proper subsets B of A . This leads to the second definition of belief function.

DEFINITION (b): The belief function associated to the basic mass assignment m , is defined as:

$$\text{Bel}(A) = \sum_{B \subseteq A} m(B). \quad (4.1)$$

NOTE: Definitions (a) and (b) are equivalent descriptions of the notion of belief function. Furthermore, the BMA that produces a given belief function is unique and can be recovered from the belief function:

$$m(A) = \sum_{B \subseteq A} (-1)^{|A-B|} \text{Bel}(B), \quad (4.2)$$

for all $A \subseteq \Theta$.

The symbol $|A|$ denotes the *cardinality* of the set A , i.e., the number of elements in A . Here, $(-1)^{|A|}$ is $+1$ if the cardinality of A is even, -1 if it is odd. This number $|A|$ is also called the *parity* of A . Furthermore, if $B \subseteq A$, then $|A - B| = |A| - |B|$ and $(-1)^{|A-B|} = (-1)^{|A|}(-1)^{|B|}$.

Also, a subset A of a frame Θ is called a *focal element* of a belief function Bel over Θ if $m(A) > 0$. The union of all the focal elements of a belief function is called its *core*.

4.4 Commonality numbers

DEFINITION: If a function $Q : 2^\Theta \rightarrow [0, 1]$ such that

$$Q(A) = \sum_{\substack{B \subset \Theta \\ A \subset B}} m(B), \quad (4.3)$$

then $Q(A)$ is called the *commonality number* for A and the function $Q(\cdot)$ is called the *commonality function* of Bel.

The relation between a belief function Bel and a commonality function Q over a frame of discernment Θ is as follows:

$$\text{Bel}(A) = \sum_{B \subset \bar{A}} (-1)^{|B|} Q(B), \quad (4.4)$$

and

$$Q(A) = \sum_{B \subset A} (-1)^{|B|} \text{Bel}(\bar{B}), \quad (4.5)$$

for all $A \subset \Theta$.

4.5 Degrees of doubt and upper probabilities

The belief function $\text{Bel}(A)$ does not reveal to what extent one doubts a proposition A , i.e., to what extent one believes its negation \bar{A} . A fuller description consists of the degree of belief $\text{Bel}(A)$ together with the *degree of doubt*

$$\text{Dou}(A) = \text{Bel}(\bar{A}), \quad (4.6)$$

then the quantity

$$\text{Pl}(A) = 1 - \text{Dou}(A), \quad (4.7)$$

which expresses the extent to which one fails to doubt A , i.e., the extent to which one finds A credible or plausible is called the *upper probability* of A .

DEFINITION: Whenever Bel is belief function over a frame Θ , the function $\text{Pl} : 2^\Theta \rightarrow [0, 1]$ defined by

$$\text{Pl}(A) = 1 - \text{Bel}(\bar{A}), \quad (4.8)$$

is called the *upper probability function* for Bel or simply plausibility function. Using (4.8) we can express $\text{Pl}(A)$ in terms of Bel's BMA m as:

$$\text{Pl}(A) = 1 - \text{Bel}(\bar{A}) \quad (4.9)$$

$$= \sum_{B \cap A \neq \emptyset} m(B). \quad (4.10)$$

Also, from (4.1) and (4.8) we can clearly notice that

$$\text{Bel}(A) \leq \text{Pl}(A). \quad (4.11)$$

Figure 4.1 shows a graphical representation of the above defined belief and plausibility. The difference

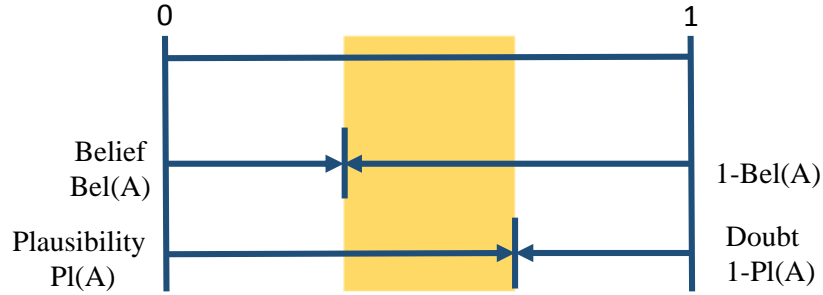


Figure 4.1: Measure of Bel, Pl and their complements along with the concept of uncertainty [28].

$\text{Pl}(A) - \text{Bel}(A)$ describes the uncertainty concerning the hypothesis A as shown in Fig.4.1 and it is represented by the evidential interval. The probability of A , i.e., $\text{Pr}(A)$ lies somewhere between $\text{Bel}(A)$ and $\text{Pl}(A)$. $\text{Bel}(A)$ represents the evidence we have for A directly and so $\text{Pr}(A)$ cannot be less than $\text{Bel}(A)$. On the other hand $\text{Pl}(A)$ represents the maximum share of the evidence that A could possibly have. Hence, $\text{Pr}(A)$ cannot be more than $\text{Pl}(A)$ and thus $\text{Pl}(A)$ is the maximum possible value of $\text{Pr}(A)$.

4.6 Bayesian belief function

DEFINITION: If Θ is a frame of discernment, then a function $\text{Bel} : 2^\Theta \rightarrow [0, 1]$ is called a *Bayesian belief function* if

1. $\text{Bel}(\phi) = 0$,
2. $\text{Bel}(\Theta) = 1$,
3. $\text{Bel}(A \cup B) = \text{Bel}(A) + \text{Bel}(B)$, whenever $A, B \subset \Theta$ and $A \cap B = \phi$

where the first three rules of Bayes's are expressed in terms of the frame of discernment. Furthermore, suppose that $\text{Bel} : 2^\Theta \rightarrow [0, 1]$ is a Bayesian belief function with plausibility or upper probability function Pl , then the following assertions are all equivalent :

- All of Bel 's focal elements are singletons.
- Bel awards a zero commonality number to any subset containing more than one element.
- $\text{Bel}(\cdot) = \text{Pl}(\cdot)$.
- $\text{Bel}(A) + \text{Bel}(\bar{A}) = 1$ for all $A \subset \Theta$ and \bar{A} denotes the complement of A .

4.7 Dempster rule of combination

One of the reasons why DST has become popular among researchers from different fields and domains is because of its combination rule. This combination rule is one of the fundamental building blocks of DST and it enables us to fuse belief masses from different independent sources but based on the same frame of reference. This combination is sometimes also referred as *orthogonal sum* of several belief functions over the same frame of reference but based on distinct bodies of evidence.

Combining two belief functions: Let there be two belief functions Bel_1 and Bel_2 , with basic mass assignment m_1 and m_2 and focal elements A_1, A_2, \dots, A_k and B_1, B_2, \dots, B_l respectively, then the combined BMA for an element or event A is given as:

$$m_{12}(A) = [m_1 \oplus m_2](A) = \frac{\sum_{\substack{i,j \\ A_i \cap B_j = A}} m_1(A_i)m_2(B_j)}{1 - k}, \quad (4.12)$$

where

$$k = \sum_{\substack{i,j \\ A_i \cap B_j = \phi}} m_1(A_i)m_2(B_j) < 1.$$

The numerator represents the accumulated evidence for the sets A_i and B_i , which supports the hypothesis A . Here, k represents the basic mass associated with conflict between different sources and $1 - k$ is introduced as a normalization factor which has the effect of completely ignoring conflict and attributing any mass associated with conflict to the null set. In particular, if it is null, it means that there is a total conflict between the sources and aggregation is then impossible. The symbol \oplus denotes Dempster combination operator. The belief function given by $m_{12}(\cdot)$ is called the orthogonal sum of Bel_1 and Bel_2 and is denoted as $\text{Bel}_1 \oplus \text{Bel}_2$. However, if $k \geq 1$, then we say that the orthogonal sum does not exist.

Combining n belief functions: Suppose there are n belief function $\text{Bel}_1, \dots, \text{Bel}_n$ over a common frame of discernment with basic mass assignment m_1, \dots, m_n . If the combined belief function $\text{Bel} = \text{Bel}_1 \oplus \dots \oplus \text{Bel}_n$ exists, then the basic mass assignment of the combined belief function Bel is given as

$$M(A) = [m_1 \oplus m_2 \oplus \dots \oplus m_n](A) = \frac{\sum_{\substack{A_1, A_2, \dots, A_n \subset 2^\Theta \\ A_1 \cap A_2 \cap \dots \cap A_n = A}} m_1(A_1) \dots m_n(A_n)}{K},$$

where

$$K = \sum_{\substack{A_1, A_2, \dots, A_n \subset 2^\Theta \\ A_1 \cap A_2 \cap \dots \cap A_n \neq \phi}} m_1(A_1) \dots m_n(A_n)$$

for all non-empty subsets of Θ . Here, K is introduced as a renormalization factor.

4.8 Illustration

In this section a step-wise illustration is provided to give an easy understanding of the different terminologies in DST.

The scenario: The given scenario discusses a robbery case that took place at a national museum, where there are three prime suspects Q, R and S out of which one is the true robber. Two expert detectives were called in to investigate the crime scene. Since there were no witness available, definite decision as to who is guilty cannot be determined nor interpreted certainly. To avoid any error regarding decision, pieces of evidence are collected, hypotheses are postulated and a DST based approach is applied to support the detectives in decision making.

Frame of Discernment: To solve the case using DST approach, the first step is defining the frame of discernment Θ whose elements are mutually exclusive and exhaustive. In the considered scenario, the only suspects available are Q, R and S , and assuming that no other offender/culprit is involved or left out the above three complete the frame. Therefore, the frame of discernment is

$$\Theta = \{Q, R, S\}$$

The corresponding power set of Θ is

$$2^\Theta = \{\phi, \{Q\}, \{R\}, \{S\}, \{Q, R\}, \{Q, S\}, \{R, S\}, \{Q, R, S\}\}.$$

Table 4.1 gives the meaning of what the subsets of 2^Θ actually signify.

Table 4.1: Interpretation of elements of 2^Θ

SET	INTERPRETATION
ϕ	No one is guilty
$\{Q\}$	Q is guilty
$\{R\}$	R is guilty
$\{S\}$	S is guilty
$\{Q, R\}$	$Q \cup R$ are guilty
$\{Q, S\}$	$Q \cup S$ are guilty
$\{R, S\}$	$R \cup S$ are guilty
$\{Q, R, S\}$	$Q \cup R \cup S$ are guilty

Basic mass assignment: At this stage, both the detectives quantify their statements by assigning weights or masses to different subsets of the power set 2^Θ . The set of elements A_k for $k = 1, \dots, 7$ is assigned to the first detective and B_k for $k = 1, \dots, 7$ to the second detective. As can be seen from the table, DST is not only concerned with singletons but also takes into account subsets such as $\{Q, R\}$, $\{Q, S\}$, $\{R, S\}$ and $\{Q, R, S\}$. Table 4.2 shows the BMAs of the two detectives. Note that there is no fixed rule in DST, that allows us to assign weights or masses to different sets or hypotheses of the power

Table 4.2: Basic mass assignment to different subsets of the power set by the two detectives

DETECTIVE 1	SET	DETECTIVE 2
$m_1(A_1) = 0.2$	$\{Q\}$	$m_2(B_1) = 0.2$
$m_1(A_2) = 0.1$	$\{R\}$	$m_2(B_2) = 0$
$m_1(A_3) = 0$	$\{S\}$	$m_2(B_3) = 0.2$
$m_1(A_4) = 0.6$	$\{Q, R\}$	$m_2(B_4) = 0$
$m_1(A_5) = 0$	$\{Q, S\}$	$m_2(B_5) = 0.4$
$m_1(A_6) = 0$	$\{R, S\}$	$m_2(B_6) = 0$
$m_1(A_7) = 0.1$	$\{Q, R, S\}$	$m_2(B_7) = 0.2$

set. In most of the cases depending on the type of situation, mass assignment is done by experts in that field or a person with great experience and may be evaluated analytically based on some observations.

Based on the basic mass assignment by both the detectives, the *belief*, *plausibility*, *commonality*, *doubt* and *disbelief* can be evaluated separately under both the detectives. For example, the *belief* for the set $\{Q, R\}$ considering the basic mass assignment of detective 1 is obtained as follows

$$\begin{aligned}
 \text{Bel}(A_4) = \text{Bel}(Q, R) &= \sum_{X \subseteq \{Q, R\}} m_1(X) \\
 &= m_1(Q) + m_1(R) + m_1(Q, R) \\
 &= 0.2 + 0.1 + 0.6 \\
 &= 0.9.
 \end{aligned}$$

Thus, *belief* in an element A of the power set is the sum of the masses of elements which are subsets of A including A itself.

On the other hand, *plausibility* of an element A is the sum of all the masses of the sets that intersect with the set A . For example, the *plausibility* for the set $\{Q, R\}$ considering basic mass assignment of detective 1 is evaluated as follows

$$\begin{aligned}
 \text{Pl}(A_4) = \text{Pl}(Q, R) &= \sum_{X \in 2^\Theta; X \cap \{Q, R\} \neq \emptyset} m_1(X) \\
 &= m_1(Q) + m_1(R) + m_1(Q, R) + m_1(Q, S) + m_1(R, S) + m_1(Q, R, S) \\
 &= 0.2 + 0.1 + 0.6 + 0.1 = 1.
 \end{aligned} \tag{4.13}$$

The corresponding measure of *doubt* is evaluated as

$$\text{Dou}(A_4) = \text{Bel}(\bar{A}_4) = 1 - \text{Pl}(A_4) = 1 - \text{Pl}(Q, R) = 1 - 1 = 0. \tag{4.14}$$

The *commonality* measure of set A_4 is evaluated as

$$\begin{aligned}
 Q(A_4) = Q(Q, R) &= \sum_{\substack{X \in 2^\Theta \\ \{Q, R\} \subseteq X}} m(X) \\
 &= m_1(Q, R) + m_1(Q, R, S) \\
 &= 0.6 + 0.1 = 0.7.
 \end{aligned}
 \tag{4.15}$$

Table 4.3 shows the *belief*, *plausibility* and *doubt* values corresponding to the basic mass assignment given in table 4.2 for both the detectives.

Table 4.3: Table showing the values for m , Bel, Pl, and Dou of different elements for both detectives.

$m(A_k)$	Bel(A_k)	Pl(A_k)	Dou(A_k)	SET	$m(B_k)$	Bel(B_k)	Pl(B_k)	Dou(B_k)
0.2	0.2	0.9	0.1	{ Q }	0.2	0.2	0.8	0.2
0.1	0.1	0.8	0.2	{ R }	0	0	0.2	0.8
0	0	0.1	0.9	{ S }	0.2	0.2	0.8	0.2
0.6	0.9	1	0	{ Q, R }	0	0.2	0.8	0.2
0	0.2	0.9	0.1	{ Q, S }	0.4	0.8	1	0
0	0.1	0.8	0.2	{ R, S }	0	0.2	0.8	0.2
0.1	1	1	0	{ Q, R, S }	0.2	1	1	0

Combining sets/hypotheses: The next step involves combining the basic mass from the two detectives for different set to obtain the combined basic mass assignment for the given propositions. In this regard, the first step is to obtain the cut set as given in table 4.4. This table highlights the sets, which are common to both A_k and B_k , i.e., $A_k \cap B_k$. The null set ϕ is used to represent the intersection of those sets of A_k and B_k having no common element.

Table 4.4: Cut set table

\cap	A_1	A_2	A_3	A_4	A_5	A_6	A_7
B_1	Q	ϕ	ϕ	Q	Q	ϕ	Q
B_2	ϕ	R	ϕ	R	ϕ	R	R
B_3	ϕ	ϕ	S	ϕ	S	S	S
B_4	Q	R	ϕ	$Q \cup R$	Q	R	$Q \cup R$
B_5	Q	ϕ	S	Q	$Q \cup S$	S	$Q \cup S$
B_6	ϕ	R	S	R	S	$R \cup S$	$R \cup S$
B_7	Q	R	S	$Q \cup R$	$Q \cup S$	$R \cup S$	Θ

To avoid mathematical effort, those columns and rows of the combination table 4.4 were dropped, which are related to non-focal elements (non-specified statements with $m(A_k) = m(B_k) = 0$). In this

Table 4.5: The reduced combinable table

\cap	A_1	A_2	A_4	A_7
B_1	Q	ϕ	Q	Q
B_3	ϕ	ϕ	ϕ	S
B_5	Q	ϕ	Q	$\{Q, S\}$
B_7	Q	R	$\{Q, R\}$	Θ

context, columns A_3, A_5, A_6 and rows B_2, B_4, B_6 are not applicable. Table 4.5 shows the reduced plot containing the combinations of focal elements exclusively.

Calculating Products and Sums of Combined Basic Assignments: As mentioned before the Dempster combination rule is given as

$$m_{12}(A) = [m_1 \oplus m_2](A) = \frac{\sum_{\substack{i,j \\ A_i \cap B_j = A}} m_1(A_i)m_2(B_j)}{1 - k}, \quad (4.16)$$

where

$$k = \sum_{\substack{i,j \\ A_i \cap B_j = \phi}} m_1(A_i)m_2(B_j).$$

From (4.16), we see that the numerator contains the sum of product of basic mass of sets which have A as a common element and A is the set whose combined basic mass is being calculated. This quantity basically denotes the total mass exactly committed to the set A . In this context, there are six instances where $A_i \cap B_j = Q$ as can be seen from the Table 4.5. Therefore, the total mass exactly committed to the set Q is

$$\begin{aligned} \sum_{\substack{i,j \\ A_i \cap B_j = Q}} m_1(A_i)m_2(B_j) &= m_1(A_1)m_2(B_1) + m_1(A_1)m_2(B_3) + m_1(A_1)m_2(B_7) + \\ &\quad m_1(A_4)m_2(B_1) + m_1(A_4)m_2(B_5) + m_1(A_7)m_2(B_1) \\ &= 0.04 + 0.08 + 0.04 + 0.12 + 0.24 + 0.02 \\ &= 0.54. \end{aligned} \quad (4.17)$$

Similarly, total mass exactly committed to the set R is

$$\sum_{\substack{i,j \\ A_i \cap B_j = R}} m_1(A_i)m_2(B_j) = m_1(A_2)m_2(B_7) = 0.02.$$

Total mass exactly committed to the set S is

$$\sum_{\substack{i,j \\ A_i \cap B_j = S}} m_1(A_i)m_2(B_j) = m_1(A_7)m_2(B_3) = 0.02.$$

Total mass exactly committed to the set $\{Q, R\}$ is

$$\sum_{\substack{i,j \\ A_i \cap B_j = \{Q,R\}}} m_1(A_i)m_2(B_j) = m_1(A_4)m_2(B_7) = 0.12.$$

Total mass exactly committed to the set $\{Q, S\}$ is

$$\sum_{\substack{i,j \\ A_i \cap B_j = \{Q,S\}}} m_1(A_i)m_2(B_j) = m_1(A_7)m_2(B_5) = 0.04.$$

Total mass exactly committed to the set $\{Q, R, S\}$ is

$$\sum_{\substack{i,j \\ A_i \cap B_j = \{Q,R,S\}}} m_1(A_i)m_2(B_j) = m_1(A_7)m_2(B_7) = 0.02.$$

Next we evaluate the value of k

$$\begin{aligned} k &= \sum_{\substack{i,j \\ A_i \cap B_j = \phi}} m_1(A_i)m_2(B_j) \\ &= m_1(A_1)m_2(B_3) + m_1(A_2)m_2(B_1) + m_1(A_2)m_2(B_3) + m_1(A_2)m_2(B_5)m_1 + (A_4)m_2(B_3) \\ &= 0.04 + 0.02 + 0.02 + 0.04 + 0.12 \\ &= 0.24. \end{aligned}$$

Therefore, $1 - k = 1 - 0.24 = 0.76$. Alternatively, we can evaluate $1 - k$ by summing all those products whose focal element is not ϕ , i.e.,

$$\begin{aligned} 1 - k &= K = \sum_{\substack{i,j \\ A_i \cap B_j \neq \phi}} m_1(A_i)m_2(B_j) \\ &= 0.04 + 0.08 + 0.04 + 0.02 + 0.12 + 0.24 + 0.12 + 0.02 + 0.02 + 0.04 + 0.02 \\ &= 0.76. \end{aligned}$$

Thus, we observe that

$$\sum_{\substack{i,j \\ A_i \cap B_j = \phi}} m_1(A_i)m_2(B_j) + \sum_{\substack{i,j \\ A_i \cap B_j \neq \phi}} m_1(A_i)m_2(B_j) = 1.$$

Table 4.6: The product table

•	A_1	A_2	A_4	A_7
B_1	0.04	$\phi : \mathbf{0.02}$	0.12	0.02
B_3	$\phi : \mathbf{0.04}$	$\phi : \mathbf{0.02}$	$\phi : \mathbf{0.12}$	0.02
B_5	0.08	$\phi : \mathbf{0.04}$	0.24	0.04
B_7	0.04	0.02	0.12	0.02

Finally, the combined basic mass assignment m_{12} of every set/hypothesis based on Dempster rule is as follows

$$m_{12}(\{Q\}) = \frac{\sum_{A_i \cap B_j = \{Q\}} m_1(A_i)m_2(B_j)}{K} = \frac{0.54}{0.76} \approx 0.7105$$

$$m_{12}(\{R\}) = \frac{\sum_{A_i \cap B_j = \{R\}} m_1(A_i)m_2(B_j)}{K} = \frac{0.02}{0.76} \approx 0.0263$$

$$m_{12}(\{S\}) = \frac{\sum_{A_i \cap B_j = \{S\}} m_1(A_i)m_2(B_j)}{K} = \frac{0.02}{0.76} \approx 0.0263$$

$$m_{12}(\{Q, R\}) = \frac{\sum_{A_i \cap B_j = \{Q, R\}} m_1(A_i)m_2(B_j)}{K} = \frac{0.12}{0.76} \approx 0.1579$$

$$m_{12}(\{Q, S\}) = \frac{\sum_{A_i \cap B_j = \{Q, S\}} m_1(A_i)m_2(B_j)}{K} = \frac{0.04}{0.76} \approx 0.0526$$

$$m_{12}(\{Q, R, S\}) = \frac{\sum_{A_i \cap B_j = \{Q, R, S\}} m_1(A_i)m_2(B_j)}{K} = \frac{0.02}{0.76} \approx 0.0263$$

Table 4.7: The basic mass assignment and the related evidence measures *belief*, *plausibility*, *commonality*, *doubt* and *uncertainty*.

2^Θ	m_{12}	Bel	Pl	Q	Dou	(Pl – Bel)
$\{Q\}$	0.7105	0.7105	0.9471	0.9474	0.0529	0.2366
$\{R\}$	0.0263	0.0263	0.2105	0.2105	0.7895	0.1842
$\{S\}$	0.0263	0.0263	0.1053	0.1053	0.8947	0.0790
$\{Q, R\}$	0.1579	0.8947	0.9737	0.1842	0.0263	0.0790
$\{Q, S\}$	0.0526	0.7895	0.9737	0.0789	0.0263	0.1842
$\{Q, R, S\}$	0.0263	1	1	0.0263	0	0

Interpretation: From Table 4.7 we see that among the singletons $\{Q\}$, $\{R\}$ and $\{S\}$, the combined basic mass m_{12} , *belief* and *plausibility* of $\{Q\}$ is the maximum. It naturally forces us to conclude

that the main culprit in the current robbery case is none other than $\{Q\}$. In fact, Bayesian or pure probabilistic approach will definitely conclude that the entire robbery has been committed by $\{Q\}$ alone. On the contrary, we also observe from Table 4.7 that the *uncertainty*, i.e., $(Pl - Bel)$ corresponding to $\{Q\}$ is the highest. Therefore, further analysis of the data in Table 4.7 is necessary to come to definite conclusion. Starting with the *uncertainty* values, even though $\{R\}$ and $\{S\}$ has low *uncertainty* values, their *belief* and *plausibility* values are also quite low and on top of that the *doubt* that either $\{R\}$ or $\{S\}$ committed the crime alone or individually is relatively high as can be seen from the table. Hence, it is highly less probable that either $\{R\}$ or $\{S\}$ is involved in the robbery individually. However, if we talk about combinations of singletons in the current interpretation, it will be unfair to decide that the combination $\{Q, S\}$ or $\{Q, R, S\}$ is involved in the crime firstly because both of their combined basic mass is quite low. Secondly due to presence of $\{S\}$ in both of them. The combined basic mass m_{12} , *belief*, and *plausibility* of $\{S\}$ is the lowest among all the possible states. On the contrary, it has the highest *doubt* value ≈ 0.8947 . Therefore, it is highly unlikely that $\{S\}$ is in any angle part of the robbery and hence we can safely neglect $\{Q, R\}$ and $\{Q, R, S\}$. Finally, the combination $\{Q, R\}$ has low *uncertainty* ≈ 0.08 and the highest combined basic mass, i.e., $m_{12}(Q, S) \approx 0.1579$ among the non-singleton sets. Furthermore, $\{Q, R\}$ also has the largest *belief* ≈ 0.8947 and *plausibility* ≈ 0.9737 . Therefore, based on the available evidence measures and its careful analysis, we can conclude that $\{Q\}$ and $\{R\}$ are combinedly guilty and there is a higher chance that they committed the entire robbery together.

Note: The above given illustration gives a detail and step wise analysis of different mathematical operations involved in DST, how they are evaluated and the decision making procedure. However, it is important to keep in mind that the decisions based on DST approach is not definite or universal in all cases and they may vary depending on the scenario of situation. Nevertheless, the above example highlights the difference in decision making process between pure probabilistic method and DST. Using Bayesian approach, we would have undoubtedly ended up with $\{Q\}$ as the culprit/thief. However, DST approach forced us to investigate the problem with much more tenacity, instead of jumping to conclusion in haste. Thus analysing the different evidence measures, we realized that even though $\{Q\}$ has the highest support values, its *uncertainty* is also comparatively high. This propelled us to look at the problem from a different dimension and since DST empowers us to include combinations of singletons also, we end up deciding in favour of $\{Q, R\}$ to be the most probable conclusion. In this illustration, the decision is highly in favour of both Q and R. However, in some cases, decision in favour of such combination is not possible when they are completely disjoint. For example, in spectrum sensing scenario, if the hypothesis denoting the absence of PU is H_0 and hypothesis denoting its presence is H_1 , then we can never decide in favour of both H_0 and H_1 , i.e., $\{H_0, H_1\}$, because that is practically not possible. One and only one of the hypotheses will be true and not both together. If we apply this rule/condition to the current case of robbery, and say that only one of them is guilty, then in that case the decision should go in favour of Q and not $\{Q, R\}$.

Chapter 5

Dempster-Shafer Theory based Cooperative Energy Detection Scheme

Equipped with the basic knowledge of DST from the previous chapter, we present the proposed CED scheme based on DST in detail in this chapter. We know that uncertainty in noise power or lack of perfect knowledge of noise variance leads to unpredictable performance of an ED trying to sense the existence of a PU. The behavior of a single ED, or a group of EDs working in collaboration for spectrum sensing has already been modeled theoretically based on pure probabilistic theory, both in the presence as well as in the absence of NU. The limitation they face in terms of SNR wall or more generalized SP wall can't be ignored as long as model uncertainties exist. Therefore, our primary motive is to examine whether it is possible to enhance the performance of the existing CED model using DST based approach. At the end, we finally observe that indeed, the proposed DST based CED is able to perform better than the traditional methods under NU.

The proposed DST based CED scheme starts with the design of BMA method, which is basically the first step of the entire scheme. The next step involves inclusion of uncertainty information into the BMA measures. These two steps form the founding pillars for the proposed scheme and are the primary reasons for performance improvement, which we will observe in the simulation section. However, there are two variants of this scheme, depending on how we model the noise variance. According to classical estimation theory, noise is treated as an unknown constant, whose true value may lie within some upper and lower bounds. On the other hand, if we move to Bayesian estimation theory, the behavior of noise variance is assumed to be a random variable with some known distribution. In this regard, we cannot use a single BMA method for different noise model. Hence based on these two noise variance model, we have proposed two different methods for evaluating BMA values and different techniques of uncertainty measurement.

5.1 Proposed scheme under unknown but constant noise variance

Fig. 5.1 shows the generalized framework for the proposed DST based CED. There are U number of SUs trying to detect the presence or absence of a single PU in a frequency band. Here, σ_{ni}^2 and ρ_i are the NU parameters associated with the i^{th} SU. The listening (sensing) channels are assumed to be AWGN

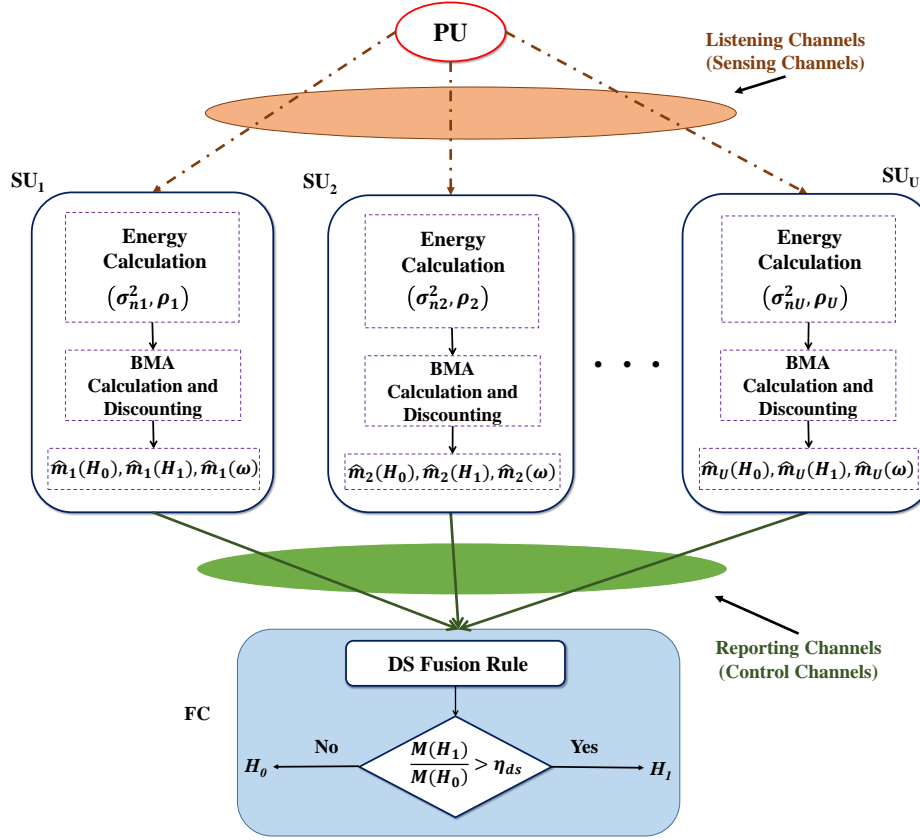


Figure 5.1: Framework for the proposed DST based CED.

channels while the reporting channels are error free. First step in this approach is estimating BMA values for different hypotheses based on the energy of the received signal. Next, to include uncertainty measure we apply the *discounting rule* of DST where the BMA values of each SU are discounted by some amount $(1 - \alpha_i)$, where α_i is called the discount rate and $(1 - \alpha_i)$ the trust value. In the final step, these discounted BMA values are used in the DST fusion rule at the FC to arrive at the global decision, which is then reported back to all the SUs via the reporting channel. These steps are explained in detail in the following subsections. Towards the end of this section, we also provide a proof for the optimality of the proposed DST based CED for the no NU case.

5.1.1 Proposed BMA method

In DST based spectrum sensing for CRs, assigning the basic mass to different hypotheses is a crucial part as the end decision heavily depends on the correctness of how the basic masses are assigned. In DST, there is no fixed rule for allocating basic mass to sets or hypotheses belonging to any case or situation. Generally, in some scenario they are assigned by experts in that particular field, or a person

with great experience or may be formulated by using some equation. Here, we propose a novel BMA method, which is based on the energy of the received signal.

In [27], the author has discussed the idea of assigning support values to different hypotheses based on probabilistic models. Consider a frame of discernment Θ , consisting of possible values of a parameter $\theta = \{\theta_0, \theta_1, \dots, \theta_k\}$. Let $\{q_{\theta_j}\}_{\theta_j \in \Theta}$ be the class of chance (or probability) densities on a set X , that models a random experiment. Furthermore, consider that if θ_j is the correct value of θ , then q_{θ_j} models the experiment. Let $x \in X$ be an observed outcome of the experiment. Since x is evidence as to which of the densities q_{θ_j} is the correct one, it is also evidence as to which element of Θ is the correct value of θ . The next step involves determining for each value of $x \in X$, a support function S_x over Θ such that $S_x(A)$ is the degree of belief/support that the observed x provides for the proposition that the true value of θ is in the subset A of Θ . In fact, in terms of probabilistic terminology, q_{θ_j} is nothing but the likelihood of θ_j and can be expressed using the likelihood function. Next, if x is a observation, then x lends plausibility to a singleton $\{\theta_j\}$ in strict proportion to the chance that q_{θ_j} assigns to x , i.e., x should determine a plausibility function Pl_x obeying [27]

$$Pl_x(\{\theta_j\}) = c \cdot q_{\theta_j}(x), \quad (5.1)$$

where c is a constant and the support function $S_x : 2^\Theta \rightarrow [0, 1]$ is given by

$$S_x(A) = 1 - Pl_x(\bar{A}). \quad (5.2)$$

In this context, for a SU performing local sensing, consider the frame of discernment $\Theta = \{\theta_0, \theta_1\} = \{H_0, H_1\}$. The power set of Θ is given as $\{\phi, H_0, H_1, \{H_0, H_1\}\}$ where $\omega = \{H_0, H_1\}$ represents the uncertainty or ignorance set. Now we observe that in the present scenario the parameter θ_j represents the hypotheses H_j for $j = 0, 1$. Also, the observation x should represent the energy value E_i at the i^{th} SU. Furthermore, $q_{\theta_j}(x)$ should be the likelihood function based on observation E_i and parameterized by H_j . Therefore, we can write $q_{\theta_j}(x) = p(E_i; H_j)$ for $j = 0, 1$, denoting the class of likelihood functions on the set of energy values $E_i \in \mathbb{R}_{\geq 0}$. Now as already discussed above if we have an observation E_i , then E_i lends plausibility to a singleton $\{H_j\} \subset \Theta$ in strict proportion to the probability that $p(E_i; H_j)$ assigns to E_i . Therefore, E_i should determine a plausibility function Pl_{E_i} as

$$Pl_{E_i}(\{H_j\}) = c \cdot p(E_i; H_j), \quad (5.3)$$

for all $H_j \in \Theta$, where c is a constant and $Pl_{E_i} : 2^\Theta \rightarrow [0, 1]$. Moreover, since the noise variance σ_i^2 is also an unknown parameter, $p(E_i; H_j)$ is further parameterized by σ_i^2 . Therefore, (5.3) can be modified as

$$Pl_{E_i}(H_j) = p(E_i; H_j, \sigma_i^2), \text{ for } j = 0, 1. \quad (5.4)$$

Hence, the plausibility for hypotheses H_0 and H_1 can be expressed as

$$\begin{aligned} Pl_{E_i}(H_0) &= c \cdot p(E_i; H_0, \sigma_i^2), \\ Pl_{E_i}(H_1) &= c \cdot p(E_i; H_1, \sigma_i^2), \end{aligned} \quad (5.5)$$

Note that c in (5.5) is a quantity that normalizes the plausibility values. Therefore, we propose c to be taken as

$$c = \frac{1}{p(E_i; H_0, \sigma_i^2) + p(E_i; H_1, \sigma_i^2)}. \quad (5.6)$$

It will be shown later in this section that this choice of c is optimal under the no NU assumption. Now using (3.8), the likelihood functions under both the hypotheses are given as

$$\begin{aligned} p(E_i; H_0, \sigma_i^2) &= \frac{1}{\sqrt{2\pi}\sigma_{0i}} \exp\left(-\frac{(E_i - \mu_{0i})^2}{2\sigma_{0i}^2}\right), \\ p(E_i; H_1, \sigma_i^2) &= \frac{1}{\sqrt{2\pi}\sigma_{1i}} \exp\left(-\frac{(E_i - \mu_{1i})^2}{2\sigma_{1i}^2}\right). \end{aligned} \quad (5.7)$$

Now the belief/support function $S_{E_i} : 2^\Theta \rightarrow [0, 1]$ is given in [27] as

$$S_{E_i}(A) = 1 - \text{Pl}_{E_i}(\bar{A}), \quad (5.8)$$

for all proper subsets $A \subseteq \Theta$. Using equations (5.5), (5.6) and (5.8) the support function for the hypothesis H_0 at the i^{th} SU is obtained as

$$\begin{aligned} S_{E_i}(H_0) &= 1 - \text{Pl}_{E_i}(H_1) \\ &= 1 - \frac{p(E_i; H_1, \sigma_i^2)}{p(E_i; H_0, \sigma_i^2) + p(E_i; H_1, \sigma_i^2)}, \\ S_{E_i}(H_0) &= \frac{p(E_i; H_0, \sigma_i^2)}{p(E_i; H_0, \sigma_i^2) + p(E_i; H_1, \sigma_i^2)}. \end{aligned} \quad (5.9)$$

Similarly support functions for H_1 and ω at the i^{th} SU is obtained as

$$S_{E_i}(H_1) = \frac{p(E_i; H_1, \sigma_i^2)}{p(E_i; H_0, \sigma_i^2) + p(E_i; H_1, \sigma_i^2)}, \quad (5.10)$$

$$S_{E_i}(\omega) = 1. \quad (5.11)$$

Now, there is a one-to-one correspondence between the set functions $m \leftrightarrow S_{E_i}$. Therefore, the BMA values for hypotheses H_0 , H_1 , and ω can be uniquely obtained from the support function S_{E_i} by means of the inversion formula [27], which is given as

$$m(A) = \sum_{B \subseteq A} (-1)^{|A-B|} S_{E_i}(B), \quad (5.12)$$

for all proper subsets $A \subseteq \Theta$. Therefore, we have

$$\begin{aligned} m_i(H_0) &= \sum_{B \subseteq H_0} (-1)^{|H_0-B|} S_{E_i}(B) \\ &= (-1)^{|H_0-H_0|} S_{E_i}(H_0) \\ &= S_{E_i}(H_0) \\ &= \frac{p(E_i; H_0, \sigma_i^2)}{p(E_i; H_0, \sigma_i^2) + p(E_i; H_1, \sigma_i^2)}, \end{aligned} \quad (5.13)$$

$$\begin{aligned}
 m_i(H_1) &= \sum_{B \subseteq H_1} (-1)^{|H_1-B|} \mathbf{S}_{E_i}(B) \\
 &= (-1)^{|H_1-H_1|} \mathbf{S}_{E_i}(H_1) \\
 &= \mathbf{S}_{E_i}(H_1) \\
 &= \frac{p(E_i; H_1, \sigma_i^2)}{p(E_i; H_0, \sigma_i^2) + p(E_i; H_1, \sigma_i^2)}, \tag{5.14}
 \end{aligned}$$

$$\begin{aligned}
 m_i(\omega) &= \sum_{B \subseteq \omega} (-1)^{|\omega-B|} \mathbf{S}_{E_i}(B) \\
 &= (-1)^{|\omega-\omega|} \mathbf{S}_{E_i}(\omega) + (-1)^{|\omega-H_0|} \mathbf{S}_{E_i}(H_0) + \\
 &\quad (-1)^{|\omega-H_1|} \mathbf{S}_{E_i}(H_1) \\
 &= 1 - \mathbf{S}_{E_i}(H_0) - \mathbf{S}_{E_i}(H_1) \\
 &= 1 - m_i(H_0) - m_i(H_1). \tag{5.15}
 \end{aligned}$$

5.1.2 BMA adjustment under NU

The BMA functions $m_i(\cdot)$ formulated above, do not take into account the amount of NU associated with the SU. As a result, the sum of $m_i(H_0)$ and $m_i(H_1)$ will always be one, i.e., $m_i(H_0) + m_i(H_1) = 1$ and consequently the basic mass for ω will be $m_i(\omega) = 0$, irrespective of presence or absence of NU. Since the quantity $m_i(\omega)$ signifies the amount of uncertainty involved with the SU, it is important that its value is non-zero under NU and zero when there is no NU. In the presence of NU, these BMA values are no longer completely reliable and as such we need some other means to incorporate the NU information in the form of $m_i(\omega)$. To achieve this, we use the *discounting rule* of DST where it provides an attractive way to discount these BMA values based on their reliability [27]. The discounting rule states that if we have a degree of trust of $1 - \alpha$ in the evidence as a whole, where $0 \leq \alpha \leq 1$, then α is adopted as a discount rate and reduce the degree of support for each proper subset A of Θ from $m(A)$ to $(1 - \alpha)m(A)$. So under NU conditions, the new BMA values for each SU will be

$$\hat{m}_i(H_0) = (1 - \alpha_i)m_i(H_0), \tag{5.16}$$

$$\hat{m}_i(H_1) = (1 - \alpha_i)m_i(H_1), \tag{5.17}$$

where α_i denotes discount rate for the i^{th} SU such that $0 \leq \alpha_i \leq 1$. Now, the BMA for ω is obtained as

$$\begin{aligned}
 \hat{m}_i(\omega) &= 1 - \hat{m}_i(H_0) - \hat{m}_i(H_1) \\
 &= 1 - (1 - \alpha_i) [m_i(H_0) + m_i(H_1)] \\
 &= 1 - (1 - \alpha_i) \\
 &= \alpha_i.
 \end{aligned}$$

Thus, we find that the BMA value for the set ω under NU, i.e., $\hat{m}_i(\omega)$ is same as the discount rate α_i . Therefore, when SUs' are subjected to NU, $\hat{m}_i(H_0) + \hat{m}_i(H_1) < 1$ and $\hat{m}_i(\omega) = \alpha_i > 0$. This

discounting factor α_i may be similar or dissimilar for different CR nodes depending on their noise variance interval. However, since $0 \leq \alpha_i \leq 1$, it is to be ensured that under any NU interval and any arbitrary nominal noise variance, the α_i value should always be confined between 0 and 1.

5.1.3 Determining discount rate α_i

Here we propose a method for determining the discount rate α_i under NU conditions. The discount rates are measured individually for every SU and as such, each SU will have its own unique discount rate α_i , depending on the NU interval associated with it. In this regard, the first piece of information required for calculating α_i is the NU parameters σ_{ni}^2 and ρ_i of each SU.

Now, considering a single energy detection based SU performing spectrum sensing under NU, the objective in NP criterion is to maximize P_{di} (probability of detection at the i^{th} SU) for a given value of P_{fi} (probability of false alarm at the i^{th} SU) $\leq \beta_i$, where β_i is the false alarm constraint at the i^{th} SU. Therefore, we have,

$$\beta_i = \max_{\sigma_i^2 \in [\sigma_{li}^2, \sigma_{ui}^2]} Q \left(\frac{\eta_i - \mu_{0i}}{\sigma_{0i}} \right) = Q \left(\frac{\eta_i - N\sigma_{ui}^2}{\sqrt{N}\sigma_{ui}^2} \right). \quad (5.18)$$

The threshold η_i for a single SU ($U=1$) under NU is then given by

$$\eta_i = \sqrt{N}\sigma_{ui}^2 Q^{-1}(\beta_i) + N\sigma_{ui}^2. \quad (5.19)$$

Thus from (5.19) we observe that the threshold η_i at the i^{th} SU is a function of β_i and upper limit of noise variance σ_{ui}^2 . Under this condition, the maximum probability of detection P_{di} is achieved, when $\sigma_i^2 = \sigma_{ui}^2$ and minimum P_{di} for $\sigma_i^2 = \sigma_{li}^2$. Now, based on threshold values evaluated from (5.19), we obtain the best case ($\sigma_i^2 = \sigma_{ui}^2$) and worst case ($\sigma_i^2 = \sigma_{li}^2$) ROC curves for one single user. Once this is estimated, we calculate α_i as the difference between the best and the worst case P_{di} values.

$$\alpha_i(\beta_i) = P_{di}(\beta_i)_{\sigma_{ui}^2} - P_{di}(\beta_i)_{\sigma_{li}^2}. \quad (5.20)$$

This technique helps us in ensuring $0 \leq \alpha_i \leq 1$. Note that with the change in nominal SNR value¹, i.e., SNR_{ni} at the CR node and sample size N , ROC curves will also change for the same NU interval $[\sigma_{li}^2, \sigma_{ui}^2]$. Therefore, we can say that α_i is a function of three parameters viz. β_i , SNR_{ni} and N . Thus (5.20) can be modified as

$$\alpha_i(N, \beta_i, \text{SNR}_{ni}) = P_{di}(N, \beta_i, \text{SNR}_{ni})_{\sigma_{ui}^2} - P_{di}(N, \beta_i, \text{SNR}_{ni})_{\sigma_{li}^2}. \quad (5.21)$$

Analytically we can express $P_{di}(N, \beta_i, \text{SNR}_{ni})_{\sigma_{ui}^2}$ and $P_{di}(N, \beta_i, \text{SNR}_{ni})_{\sigma_{li}^2}$ in equation (5.21) as

$$\begin{aligned} P_{di}(N, \beta_i, \text{SNR}_{ni})_{\sigma_{ui}^2} &= \max_{\sigma_i^2 \in [\sigma_{li}^2, \sigma_{ui}^2]} Q \left(\frac{\eta_i - \mu_{1i}}{\sigma_{1i}} \right) \\ &= Q \left(\frac{\eta_i - N\sigma_{ni}^2(\rho_i + \text{SNR}_{ni})}{\sqrt{N}\sigma_{ni}^2(\rho_i + \text{SNR}_{ni})} \right) \end{aligned} \quad (5.22)$$

¹ Since only the NU interval is known to us and not the exact value of noise variance, therefore, it is never possible to know the true SNR value at the SU. Hence, the nominal SNR is utilized for the evaluation of α_i values.

and

$$\begin{aligned}
 P_{di}(N, \beta_i, \text{SNR}_{ni})_{\sigma_{1i}^2} &= \min_{\sigma_i^2 \in [\sigma_{1i}^2, \sigma_{2i}^2]} Q\left(\frac{\eta_i - \mu_{1i}}{\sigma_{1i}}\right) \\
 &= Q\left(\frac{\eta_i - N\sigma_{ni}^2\left(\frac{1}{\rho_i} + \text{SNR}_{ni}\right)}{\sqrt{N}\sigma_{ni}^2\left(\frac{1}{\rho_i} + \text{SNR}_{ni}\right)}\right). \tag{5.23}
 \end{aligned}$$

Using (5.22) and (5.23) in (5.21), α_i can be expressed in closed form as

$$\alpha_i(N, \beta_i, \text{SNR}_{ni}) = Q\left(\frac{\eta_i - N\sigma_{ni}^2(\rho_i + \text{SNR}_{ni})}{\sqrt{N}\sigma_{ni}^2(\rho_i + \text{SNR}_{ni})}\right) - Q\left(\frac{\eta_i - N\sigma_{ni}^2\left(\frac{1}{\rho_i} + \text{SNR}_{ni}\right)}{\sqrt{N}\sigma_{ni}^2\left(\frac{1}{\rho_i} + \text{SNR}_{ni}\right)}\right), \tag{5.24}$$

where the value of η_i is obtained from (5.19). Fig. 5.2 shows the plot of α_i for different NU intervals as a function of β_i and $\text{SNR}_n(\text{dB}) = -5$ dB. It can be clearly seen that with the increase in NU interval the α_i or discount rate of a SU also increases. For false alarm rate $\beta_i = 0.1$, the α_i values intersecting the black dotted line denotes the discount rate to be used depending on the NU interval associated with the SU.

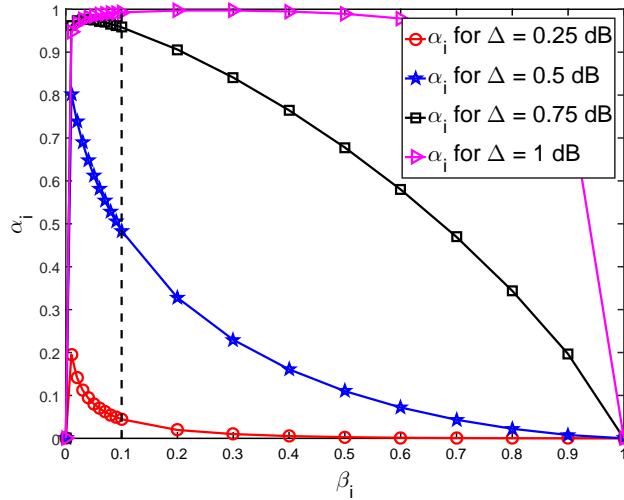


Figure 5.2: Plot of α_i for different NU intervals as a function of β_i , $\text{SNR}_n(\text{dB}) = -5$ dB and $N = 300$ for different values of noise uncertainty interval Δ .

Here, in order to calculate the discount rate α_i for each SU, for convenience we have assumed the β_i to be same as the false alarm value used at the FC. Therefore, we can write $\beta_i = \beta$. However, note that the SUs do not make any local decisions and the value $\beta_i = \beta$ is only used for α_i calculation.

5.1.4 Data fusion at the FC

The BMA adjustment is performed locally at the SU with the corresponding discount rate α_i . For identical CR nodes we can assume $\alpha_1 = \alpha_2 = \dots = \alpha_U = \alpha$. But if the NU interval is different

for each SU_i then the discount rates will also differ accordingly. The discounted BMA values are then sent to the FC via the reporting channel. In the FC, Dempster combination rule is used to fuse the BMA values from all the U SUs, which gives us the combined basic mass $M(H_0)$ and $M(H_1)$ for hypothesis H_0 and H_1 respectively,

$$\begin{aligned} M(H_0) &= \frac{1}{K} \sum_{A_1 \cap A_2 \cap \dots \cap A_U = H_0} \prod_{i=1}^U \hat{m}_i(A_i), \\ M(H_1) &= \frac{1}{K} \sum_{A_1 \cap A_2 \cap \dots \cap A_U = H_1} \prod_{i=1}^U \hat{m}_i(A_i). \end{aligned} \quad (5.25)$$

Finally, the test statistic at the FC is taken as the ratio of $M(H_1)$ and $M(H_0)$

$$T_{ds} = \frac{M(H_1)}{M(H_0)} \underset{H_0}{\overset{H_1}{\geq}} \eta_{ds}, \quad (5.26)$$

where η_{ds} is the threshold under DST scheme at FC. In this context, the threshold η_{ds} is a function of β and SNR_{ni} value at the individual CR nodes. For determining threshold η_{ds} , we take $\alpha_i = 0$ to ensure that the constraint $P_{fa} \leq \beta$ is maintained for all values of α_i .

5.1.5 Optimality of the proposed scheme in the absence of NU

In the presence of NU, it is difficult to justify the optimality of the proposed DST scheme. However, we show that under no NU condition, i.e., $\Delta = 0$, the proposed DST based fusion rule boils down to the optimal fusion rule of likelihood ratio (LR). Note for $\Delta_i = 0$ dB, $\forall i$, we have $\sigma_{li}^2 = \sigma_{ui}^2, \forall i$, which along with (5.21) means that $\alpha_i = 0, \forall i$. Therefore, for this case $\hat{m}_i(\omega) = 0, \hat{m}_i(H_0) = m_i(H_0)$ and $\hat{m}_i(H_1) = m_i(H_1)$ for $i = 1, \dots, U$ so that the test statistic T_{ds} in (5.26) becomes

$$\begin{aligned} T_{ds} &= \frac{M(H_1)}{M(H_0)} = \frac{\frac{1}{K} \prod_{i=1}^U m_i(H_1)}{\frac{1}{K} \prod_{i=1}^U m_i(H_0)} \\ &= \prod_{i=1}^U \frac{\frac{p(E_i; H_1, \sigma_i^2)}{p(E_i; H_0, \sigma_i^2) + p(E_i; H_1, \sigma_i^2)}}{\frac{p(E_i; H_0, \sigma_i^2)}{p(E_i; H_0, \sigma_i^2) + p(E_i; H_1, \sigma_i^2)}} \\ &= \prod_{i=1}^U \frac{p(E_i; H_1, \sigma_i^2)}{p(E_i; H_0, \sigma_i^2)}, \end{aligned} \quad (5.27)$$

which is the optimal LR test statistic for the binary hypothesis testing problem in (3.9) [72]. Therefore, the detection performance of tests with T_{sum} and T_{ds} will have same performance in the absence of NU ($\Delta = 0$) which will mean that $\alpha_i = 0, \forall i$, i.e., there is no discounting.

5.2 Simulation results under unknown but constant noise variance

The simulation results are divided into three main parts. In the first part, performance analysis of the proposed DST scheme is done in terms of P_d vs $\text{SNR}_n(\text{dB})$ plots and receiver operating characteristics (ROC) curves considering homogeneous CR nodes. In the second part, performance comparison of the proposed DST based CED is carried out with the traditional sum fusion rule. In the third and final part, generalized SNR wall (or SP wall) results are presented for the sum fusion rule in different scenarios followed by comparison with DST based CED.

For our simulations, we assumed that the PU signal is a zero-mean complex and circularly symmetric Gaussian signal. NP detector is assumed with the constraint on the false alarm probability of β . Generally in a practical scenario, σ_i^2 of each SU can take any value within the limits $[\sigma_{li}^2, \sigma_{ui}^2]$. However, for the NP criterion, the key objective under NU is to ensure that for low SNR values the constraint $P_{fa} \leq \beta$ is maintained at all times. In order to achieve this constraint, the threshold at FC for both the schemes (i.e. sum and DST) is determined by setting the true value of all SUs to the upper limit of noise variance, i.e., $\sigma_i^2 = \sigma_{ui}^2, \forall i$, for a fixed value of β . Also for the threshold estimation under H_0 , the discount rate α_i is set to 0, i.e., $\alpha_i = 0, \forall i$ since we chose $\sigma_i^2 = \sigma_{ui}^2$ and σ_{ui}^2 is exactly known to us. On the contrary, for performance analysis and comparison of sum and DST under NU, the true noise variance used for the experiments is the lower noise variance limit, i.e., $\sigma_i^2 = \sigma_{li}^2$ and the discount rate $\alpha_i \neq 0$. This corresponds to the worst case scenario where the detector has been designed to maintain the false alarm constraint even for the highest allowed noise variance while the actual noise variance is the lowest allowed value of noise variance. Unless stated otherwise, the number of cooperating SUs is $U = 3$, the number of received observations used for evaluating received signal energy is $N = 300$ while the number of realizations used for estimating the probability of detection is 10,000.

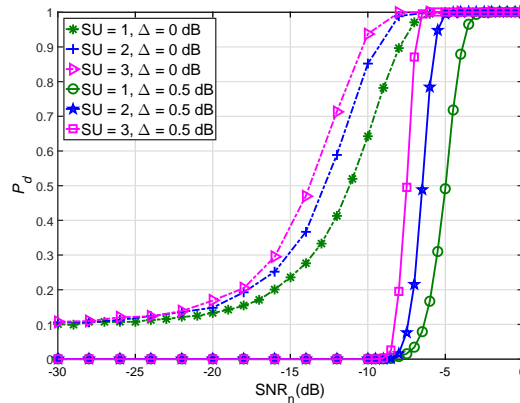


Figure 5.3: P_d vs $\text{SNR}_n(\text{dB})$ plots of DST scheme for homogeneous case with different number of SUs in the presence ($\Delta = 0.5$ dB) and absence ($\Delta = 0$ dB) of NU. Here, $\beta_i = \beta = 0.1$.

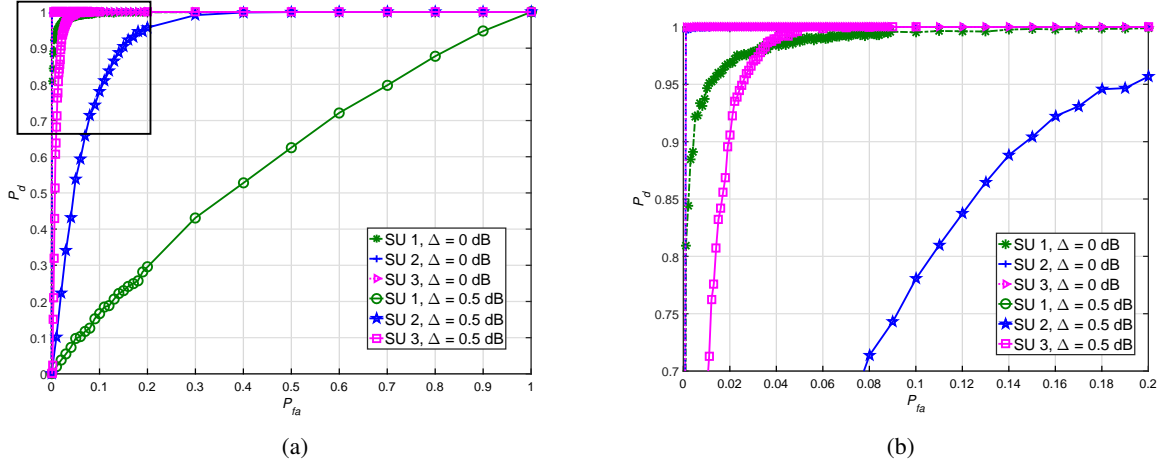


Figure 5.4: (a) ROC curves for the proposed DST based CED for homogeneous case considering different number of participating SUs in the presence ($\Delta = 0.5$ dB) and absence ($\Delta = 0$ dB) of NU at $\text{SNR}_n(\text{dB}) = -6$ dB. (b) Zoomed portion of figure (a).

5.2.1 Performance analysis of the proposed DST scheme

For the proposed DST scheme, deriving the distribution of the test statistic T_{ds} under both the hypotheses is non-trivial and tedious, as such, the threshold η_{ds} is evaluated empirically. Note that the empirical evaluation of threshold can be done off-line as it depends on all the known parameters such noise variance $\sigma_i^2 = \sigma_{ui}^2$, β , and nominal $\text{SNR}(\text{dB})$. Fig. 5.3 shows the P_d vs $\text{SNR}_n(\text{dB})$ plots of DST scheme for $\beta = 0.1$ considering different number of participating SUs. Fig. 5.4 presents the ROC curves for the same scheme at $\text{SNR}_n(\text{dB}) = -6$ dB. It can be clearly observed from both the plots that with increase in the number of SUs, the performance of DST scheme improves significantly, which validates the fact that the proposed scheme has the property of cooperative gain in the presence as well as in the absence of the NU.

5.2.2 Performance comparison of DST and sum fusion rule

5.2.2.1 Homogeneous SUs

As already mentioned earlier, for the homogeneous case, the NU parameters are identical for all SUs. Fig. 5.5 (a) shows the performance comparison of the proposed DST fusion rule to that of the sum fusion rule in terms of P_d vs $\text{SNR}_n(\text{dB})$ plots for different NU intervals of $\Delta = 0, 0.5$ and 1 dB. The nominal variance at each SU for this plot is considered to be $\sigma_n^2 = 1$. First observation from the figure is that under no NU ($\Delta = 0$), the performances of both fusion rules overlap. Note that $\Delta = 0$ results in $\alpha = 0$ and in line with our earlier discussion both the test statistics T_{sum} and T_{ds} are equivalent to the optimal LR test statistic for $\alpha = 0$, resulting in the same performance. Second observation from the figure is that for NU of $\Delta = 0.5$ dB and $\Delta = 1$ dB, performances of both the fusion rules degrade. However, proposed DST based approach significantly outperforms the traditional sum fusion rule in the

presence of NU. Similar results can be observed from fig. 5.5 (b), which presents the ROC comparison of DST and sum based CED scheme for $\Delta = 0$ dB and $\Delta = 0.5$ dB for $\text{SNR}_n(\text{dB}) = -6$ dB and number of SU, $U = 3$.

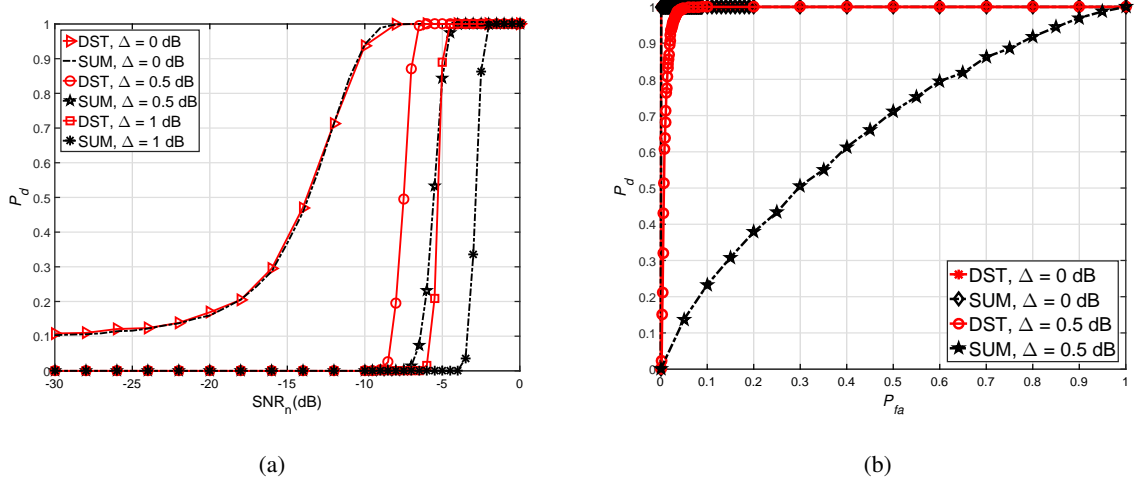


Figure 5.5: (a) P_d vs $\text{SNR}_n(\text{dB})$ comparison between the proposed DST and the sum fusion rule for CED with homogeneous SU nodes. Here $U = 3$ and $\beta = 0.1$. (b) Comparison of ROCs for DST and sum based CED schemes for $\text{SNR}_n(\text{dB}) = -6$ dB under homogeneous NU parameters $\Delta = 0, \Delta = 0.5$ dB, with $\sigma_n^2 = 1$ and number of SU, $U = 3$.

5.2.2.2 Heterogeneous CR nodes

For the case of heterogeneous CR nodes, we have considered the most generalized scenario, where each SU has a unique nominal noise variance σ_{ni}^2 and uncertainty factor ρ_i , which determines the uncertainty interval. The number of SUs is taken as $U = 3$. For simulation purpose, it is assumed that the first SU has a NU interval of $\Delta_1 = 0.25$ dB, the second SU has $\Delta_2 = 0.5$ dB, and the third SU has $\Delta_3 = 1$ dB. The nominal noise variances for the three SUs are taken as $\sigma_{n1}^2 = 0.9$, $\sigma_{n2}^2 = 1$ and $\sigma_{n3}^2 = 1.1$. Fig. 5.6 (a) shows the P_d vs P (log scale) plot comparison between the DST and the sum rule for $\beta = 0.1$ and Fig. 5.6 (b) shows the ROC curves for both the schemes at average signal power of $P = 0.3$. It can be clearly observed from both these plots that, even for heterogeneous NU intervals for different SUs, the proposed DST based CED scheme is performing much better than the usual sum rule based CED method.

Note : This set up is considered to visualize/simulate the worst case scenario when the noise variance used to set the threshold, i.e., σ_{ui}^2 , and σ_{li}^2 , which is used to simulate the P_d vs SNR plots are extremely far apart. Hence, during P_d vs $\text{SNR}_n(\text{dB})$ simulation, the P_d curves do not maintain the false alarm constraint for very low SNR values. The main purpose of considering σ_{ui}^2 for threshold estimation is

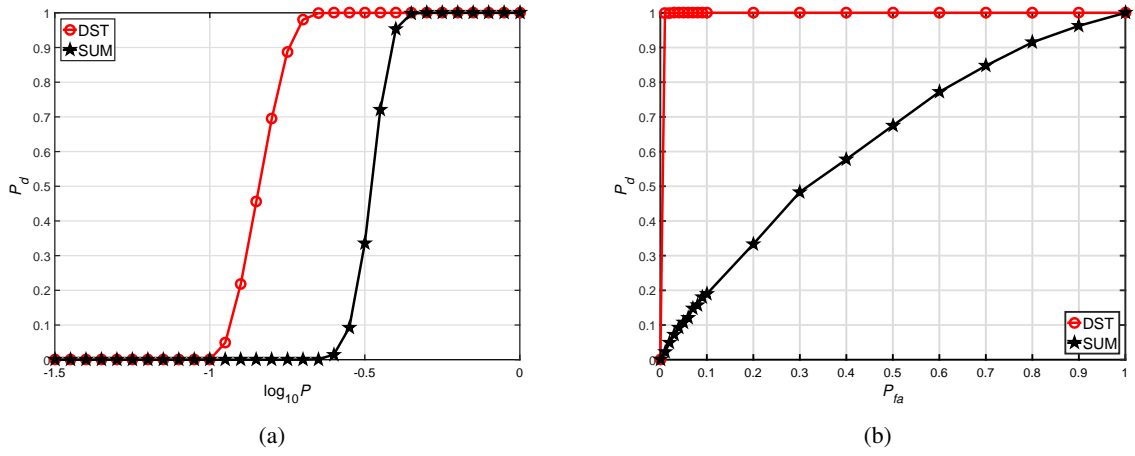


Figure 5.6: (a) P_d vs P (log scale) comparison for CED under generalized heterogeneous NU parameters. (b) ROC Comparison of DST and sum based CED schemes for average signal power, $P = 0.3$ under generalized heterogeneous NU parameters.

primarily to restrict the false alarm probability to always satisfy the constraint of $\boxed{P_{fa} \leq \beta}$, for any value of σ_i^2 within the limits $[\sigma_{li}^2, \sigma_{ui}^2]$. Fig. 5.7 shows the P_d vs SNR_n (dB) plots for different values of true noise variance σ_i^2 . Here, $\Delta = 0.5$ dB, false alarm constraint $\beta = 0.1$, number of SU, $U = 3$ and $\sigma_{ni}^2 = 1 \forall i$. The thresholds are evaluated by setting $\sigma_i^2 = \sigma_{ui}^2 \forall i$. Thus, as the true value of σ_i^2 gets closer towards the upper noise limit σ_{ui}^2 , the P_d curve at low SNR region approaches the actual constraint of β .

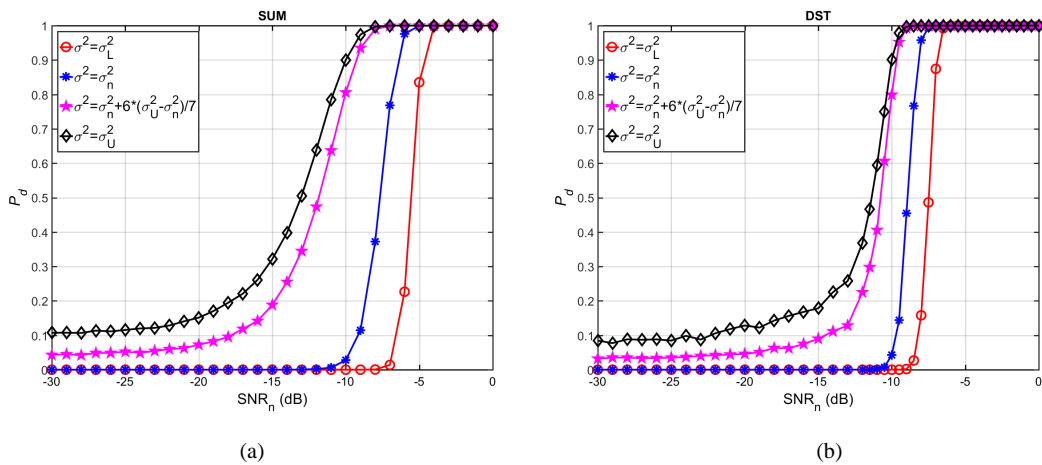


Figure 5.7: (a) P_d vs SNR_n (dB) plot of sum fusion rule for different values of σ_i^2 . (b) P_d vs SNR_n (dB) plot of DST fusion rule for different values of σ_i^2 . σ_L^2 denotes the lower limit of noise variance and σ_U^2 the upper limit.

5.3 Proposed DST based CED under random noise variance

In the previous section, we designed the DST based CED scheme considering the noise to be an unknown constant and assuming that all the SUs in the CR network are heterogeneous, i.e., having different NU parameters. In this section, we will present the DST based CED scheme considering noise as a random variable having a known distribution. The heterogeneous nature of the participating SUs in the CR network is maintained, i.e., the distribution parameters of noise variance may be different for different SUs or the SUs may have entirely different probability model for noise variance.

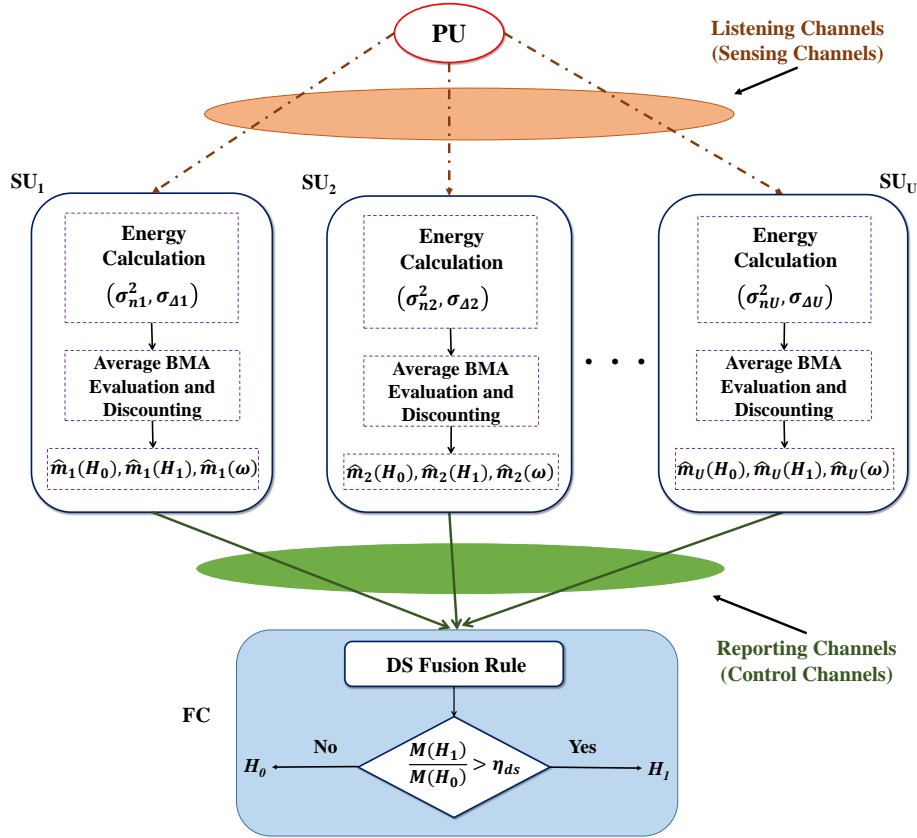


Figure 5.8: Framework for the proposed DST based CED.

5.3.1 BMA method under random noise variance

Considering the same frame of reference for a SU performing local sensing as $\Theta = \{H_0, H_1\}$, where H_0 denotes the hypothesis that the PU is absent and H_1 hypothesis denotes its presence. Then the power set of Θ is given as $\{\phi, H_0, H_1, \{H_0, H_1\}\}$, where ϕ is a null set and $m(\phi) = 0$, while the $\omega = \{H_0, H_1\}$ represents the uncertainty or ignorance set.

In the previous DST based CED scheme where we treated noise-variance as an unknown constant, we proposed the following BMA functions for hypotheses H_0 , H_1 and ω

$$\begin{aligned} m_i(H_0) &= \frac{p(E_i; H_0, \sigma_i^2)}{p(E_i; H_0, \sigma_i^2) + p(E_i; H_1, \sigma_i^2)}, \\ m_i(H_1) &= \frac{p(E_i; H_1, \sigma_i^2)}{p(E_i; H_0, \sigma_i^2) + p(E_i; H_1, \sigma_i^2)}, \\ m_i(\omega) &= 1 - m_i(H_0) - m_i(H_1), \end{aligned} \quad (5.28)$$

where $p(E_i; H_j, \sigma_i^2)$ are likelihood functions parameterized by H_j and also by the unknown constant σ_i^2 . The likelihood functions $p(E_i; H_j; \sigma_i^2)$ for $j = 0, 1$ are expressed as

$$p(E_i; H_0, \sigma_i^2) = \frac{1}{\sqrt{2\pi}\sigma_{0i}} \exp\left(-\frac{(E_i - \mu_{0i})^2}{2\sigma_{0i}^2}\right), \quad (5.29)$$

$$p(E_i; H_1, \sigma_i^2) = \frac{1}{\sqrt{2\pi}\sigma_{1i}} \exp\left(-\frac{(E_i - \mu_{1i})^2}{2\sigma_{1i}^2}\right). \quad (5.30)$$

We showed that these choices of BMA for H_0 and H_1 along with DST fusion at the FC, results in optimal detection performance similar to using likelihood ratio test (LRT) statistics for the binary hypothesis testing problem in (3.8) under no NU condition. However, when noise power is not an unknown deterministic quantity but a random variable, the appropriate way of expressing the likelihood function is

$$p(E_i|\sigma_i^2; H_0) = \frac{1}{\sqrt{2\pi}\sigma_{0i}} \exp\left(-\frac{(E_i - \mu_{0i})^2}{2\sigma_{0i}^2}\right), \quad (5.31)$$

$$p(E_i|\sigma_i^2; H_1) = \frac{1}{\sqrt{2\pi}\sigma_{1i}} \exp\left(-\frac{(E_i - \mu_{1i})^2}{2\sigma_{1i}^2}\right). \quad (5.32)$$

The symbol “|” has been used to signify that in the current scenario, the noise variance is a random variable, hence, the likelihood functions $p(E_i|\sigma_i^2; H_j)$ are “conditioned” on σ_i^2 and parameterized by H_j for $j = 0, 1$. However, in order to compute the BMA values we have to calculate the average of $p(E_i|\sigma_i^2; H_0)$ and $p(E_i|\sigma_i^2; H_1)$, which can be evaluated as

$$p'(E_i; H_0) = \int_{-\infty}^{\infty} p(E_i|\sigma_i^2; H_0) f(\sigma_i^2) d\sigma_i^2, \quad (5.33)$$

$$p'(E_i; H_1) = \int_{-\infty}^{\infty} p(E_i|\sigma_i^2; H_1) f(\sigma_i^2) d\sigma_i^2. \quad (5.34)$$

By substituting $p(E_i; H_j, \sigma_i^2)$ with $p'(E_i; H_j)$ for $j = 0, 1$ in (5.28), we get

$$m_i'(H_0) = \frac{p'(E_i; H_0)}{p'(E_i; H_0) + p'(E_i; H_1)} \quad (5.35)$$

and

$$m'_i(H_1) = \frac{p'(E_i; H_1)}{p'(E_i; H_0) + p'(E_i; H_1)}, \quad (5.36)$$

while the BMA for ω is given by

$$m'_i(\omega) = 1 - m'_i(H_0) - m'_i(H_1). \quad (5.37)$$

Thus, we observe that when the noise variance is modeled as a random variable with a known distribution $f(\sigma_i^2)$, we have to evaluate the average BMA values.

5.3.2 BMA adjustment under NU

Similar to the earlier case, the average BMA method do not take into account the uncertainty information. Therefore, the sum of $m'_i(H_0)$ and $m'_i(H_1)$ will always be one i.e. $m'_i(H_0) + m'_i(H_1) = 1$ and $m'_i(\omega)$ will always be equal to 0. To incorporate NU data or specifically determining the support value for $m'_i(\omega)$, the BMAs of each SU are discounted before sending them to FC by using the DST discounting rule. So under NU conditions the new BMAs for each SU will be,

$$\hat{m}_i(H_0) = (1 - \alpha_i)m'_i(H_0), \quad (5.38)$$

$$\hat{m}_i(H_1) = (1 - \alpha_i)m'_i(H_1), \quad (5.39)$$

where α_i denotes discount rate for i^{th} SU. In this case $\hat{m}_i(H_0) + \hat{m}_i(H_1) < 1$, therefore the support for $\hat{m}_i(\omega)$ is obtained as

$$\begin{aligned} \hat{m}_i(\omega) &= 1 - \hat{m}_i(H_0) - \hat{m}_i(H_1) \\ &= 1 - (1 - \alpha_i) [m'_i(H_0) + m'_i(H_1)] \\ &= 1 - (1 - \alpha_i) \\ \hat{m}_i(\omega) &= \alpha_i. \end{aligned} \quad (5.40)$$

Thus, even in the case of random noise variance, we find that the basic mass for uncertainty set $\hat{m}_i(\omega)$ is same as the discount rate α_i .

5.3.3 Determining discount rate α_i under random noise variance

In the previous classical model of noise variance, we evaluated the discount rate as the difference between the best case and worst case ROC curves for a given value of false alarm constraint $\beta_i = \beta$. To compute those ROC curves we took advantage of our knowledge of noise variance interval. Determining the threshold based on upper limit of noise variance, the best case ROC was obtained by setting $\sigma_i^2 = \sigma_{ui}^2$ and the worst case ROC for $\sigma_i^2 = \sigma_{li}^2$. Finally, the discount rate α_i for a fixed nominal SNR and β_i was computed as

$$\alpha_i(\beta_i, \text{SNR}_{ni}) = P_{di}(\beta_i, \text{SNR}_{ni})_{\sigma_{ui}^2} - P_{di}(\beta_i, \text{SNR}_{ni})_{\sigma_{li}^2}.$$

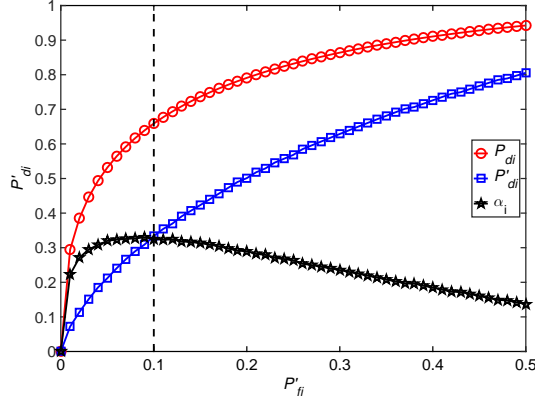


Figure 5.9: The discounting rate α_i , as a function of constraint on the false alarm probability for ASNR (dB) = -10 dB. For $\beta_i = \beta = 0.1$, the discount rate α_i is the point where the dotted line intersects the α_i curve.

However, in the current scenario of Bayesian approach, the noise variance is modeled as a random variable and as such no information is available regarding its interval. So we propose a different method for determining discount rate α_i while maintaining the fact that the discount rates are unique for each SU and its value depends on the distribution of noise variance associated with the SU. Similar to the earlier case, to determine α_i , we take the help of the ROC curves for normal energy detection at i^{th} SU based on NP criterion. The key idea is that each SU has its own ROC curve when σ_i^2 is exactly known, i.e., when there is no NU. We denote this ROC as true P_{di} . Also, it has a ROC curve when σ_i^2 is a random quantity, which is termed as average P_{di} and denoted by P'_{di} . Both these ROC curves can be obtained via theoretical calculations. The discount rate, α_i of i^{th} SU is evaluated as the difference between true P_{di} and average P_{di} , i.e., P'_{di} , for a particular false alarm rate, β_i . For convenience, we have assumed the value of β_i to be same as β of FC. Therefore, α_i can be expressed as

$$\alpha_i(\beta, \text{ASNR}) = P_{di}(\beta, \text{ASNR}) - P'_{di}(\beta, \sigma_{\Delta}^2, \text{ASNR}), \quad (5.41)$$

where true P_{di} is calculated using equation (3.12) and average P_{di} is calculated using equation (3.22). Therefore, we can also express (5.41) as

$$\alpha_i(\beta, \text{ASNR}) = Q\left(\frac{\eta_{sum} - \mu_1}{\sigma_1}\right) - \int_0^{\infty} Q\left(\frac{\eta'_{sum} - \mu_1}{\sigma_1}\right) f(\sigma_i^2) d\sigma_i^2. \quad (5.42)$$

Here, η_{sum} is the threshold of sum rule based CED under no NU condition and η'_{sum} is the threshold of sum rule based CED in the presence of NU. Fig.5.9 shows the discounting rate α_i as a function of constraint on the false alarm probability at ASNR (dB) = -10 dB. The noise variance σ_i^2 in this case is assumed to be Gaussian distributed with mean, $\sigma_n^2 = 1$ and variance, $\sigma_{\Delta}^2 = 0.01$.

5.3.4 Data fusion at the FC

The discounting method described above is performed at the individual SU. The average BMA values $m'_i(H_0)$ and $m'_i(H_1)$ of each SU_i are adjusted with the corresponding discount rate α_i associated with it. For identical CR nodes we can assume $\alpha_1 = \alpha_2 = \dots = \alpha_U = \alpha$. However, if the SUs' have different noise variance distribution and distribution parameters, then in that case the discount rates of each SU will also vary accordingly. The BMA adjustment is done according to the equations (5.38) and (5.39). These discounted BMAs are sent to FC for fusion. The DS combination rule is used to fuse the BMAs from the U SUs, which gives us the total support $M(H_0)$ and $M(H_1)$ for hypothesis H_0 and H_1 as given by . Similarly, the test statistic at the FC is taken as

$$T_{ds} = \frac{M(H_1)}{M(H_0)} \underset{H_0}{\overset{H_1}{\geq}} \eta_{ds}, \quad (5.43)$$

where η_{ds} is the threshold at FC under DST scheme.

5.4 Simulation results under random noise variance

The key objective in this section is to compare the performance of proposed DST based CED scheme with that of the sum based CED under random noise-variance. For convenience, we consider all the SUs to have identical noise variance distribution and distribution parameters. For our simulations, we assume that the PU signal is a complex and circular symmetric Gaussian signal. The number of cooperating SUs is $U = 5$, the number of received observations used for evaluating received signal energy is $N = 300$ while the number of realizations used for estimating the probability of detection is 10,000. The nominal noise variance is chosen as $\sigma_n^2 = 1$. Two different values of σ_Δ^2 are taken into account, $\sigma_\Delta^2 = 0.01$ and $\sigma_\Delta^2 = 0.02$ for performance evaluation. For P'_d vs ASNR (dB) simulations, the false alarm constraint at FC, i.e., β , is chosen as $\beta = 0.1$. For ROC curves simulation ASNR (dB) of -10 dB is fixed. As deriving the distribution of T_{ds} under both the hypotheses is non-trivial and tedious, the threshold η_{ds} is evaluated empirically under H_0 for each value of ASNR (dB) such that the P_{fa} constraint of $\beta = 0.1$ is always satisfied at FC. Note that the empirical evaluation of threshold can be done off-line as it depends on all the known parameters such as the pdf of the noise variance, $\beta = 0.1$ and ASNR (dB). Moreover, during threshold estimation under H_0 , the discount rate $\alpha_i \neq 0$ and is determined from (5.42). This is because in this case, noise variance is a random variable and cannot be set to some fixed constant.

Fig. 5.10 (a) presents P'_d vs ASNR (dB) while Fig. 5.10 (b) shows the ROC curves comparison of DST and sum based CED schemes for Gaussian distributed noise variance. From both the figures, it can be clearly observed that in the absence of NU, the performance of both schemes overlap. On the other hand, in the presence of NU, there is degradation in the performance of both CED schemes. However, the degradation in the performance of the sum fusion rule is significantly higher as compared to that of proposed DST based fusion even for small NU values of $\sigma_\Delta^2 = 0.01$ and $\sigma_\Delta^2 = 0.02$.

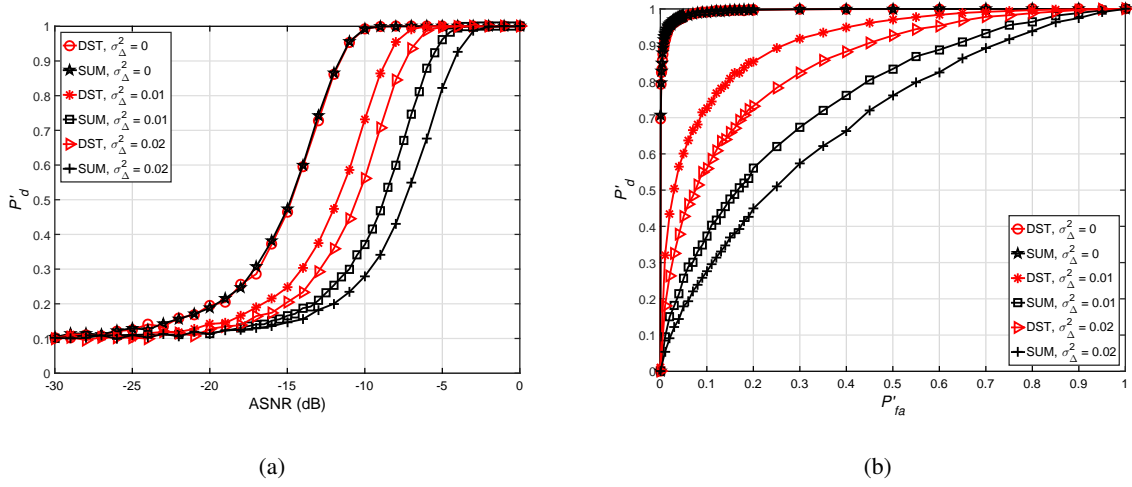


Figure 5.10: (a) P'_d as a function of ASNR (dB) for $\beta = 0.1$ considering σ_w^2 as a Gaussian distributed random variable. (b) ROC curves comparison at ASNR (dB) = -10 dB considering σ_w^2 as a Gaussian distributed.

Similarly, Fig. 5.11 (a) and 5.11 (b) show P'_d vs ASNR (dB) and ROC comparison of the two schemes where noise variance is modeled as a uniformly distributed random variable. Even for this case the proposed DST scheme outperforms sum for both values of $\sigma_\Delta^2 = 0.01$ and $\sigma_\Delta^2 = 0.02$.

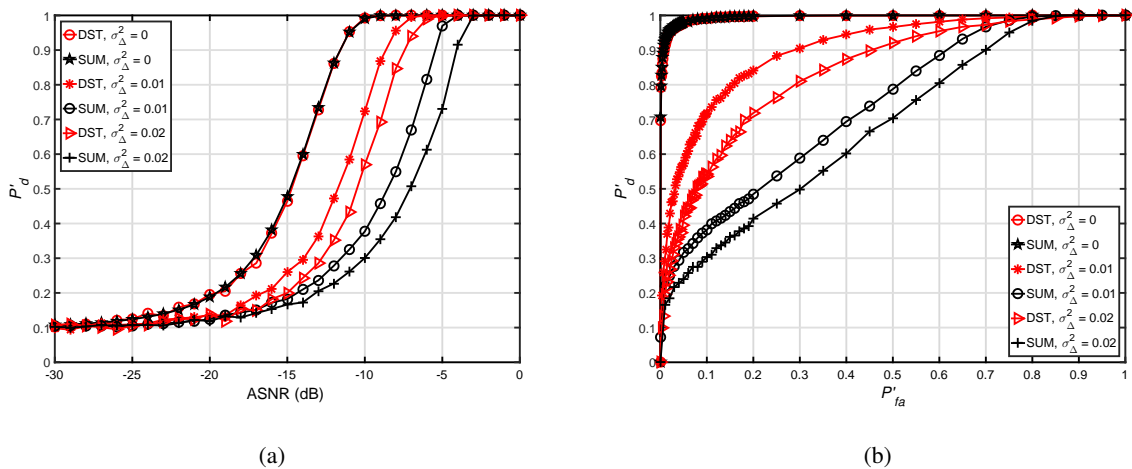


Figure 5.11: (a) P'_d as a function of ASNR (dB) for $\beta = 0.1$ considering σ_w^2 as a uniformly distributed random variable. (b) ROC curves comparison at ASNR (dB) = -10 dB considering σ_w^2 as a uniformly distributed random variable

5.5 Comparison between DST and sum in terms of SNR and SP walls

In chapter 3, we demonstrated the existence of generalized SNR/SP wall phenomenon in the case of sum rule based CED in the presence of NU. The SNR wall concept was discussed considering the first NU model where noise variance is assumed to be a unknown but deterministic constant. In this section, same simulations are performed to find the existence of SP/SNR wall for the proposed DST based CED scheme. For simulating the environment, we choose the same NU parameters of table 5.1 for the 4 different cases.

Table 5.1: Considered cases for SP wall simulation and comparison between DST and sum rule CED.

Case	NU parameters ($U = 3$)
I	$\sigma_{n1}^2 = \sigma_{n2}^2 = \sigma_{n3}^2 = 1$ $\Delta_1 = \Delta_2 = \Delta_3 = 0.75$ dB $\rho_1 = \rho_2 = \rho_3 = 1.189$
II	$\sigma_{n1}^2 = 0.9, \sigma_{n2}^2 = 1, \sigma_{n3}^2 = 1.1$ $\Delta_1 = \Delta_2 = \Delta_3 = 1$ dB $\rho_1 = \rho_2 = \rho_3 = 1.259$
III	$\sigma_{n1}^2 = \sigma_{n2}^2 = \sigma_{n3}^2 = 1$ $\Delta_1 = 0.5, \Delta_2 = 0.75, \Delta_3 = 1$ dB $\rho_1 = 1.122, \rho_2 = 1.188, \rho_3 = 1.259$
IV	$\sigma_{n1}^2 = 0.9, \sigma_{n2}^2 = 1, \sigma_{n3}^2 = 1.1$ $\Delta_1 = 0.25, \Delta_2 = 0.5, \Delta_3 = 1$ dB $\rho_1 = 1.0593, \rho_2 = 1.122, \rho_3 = 1.259$

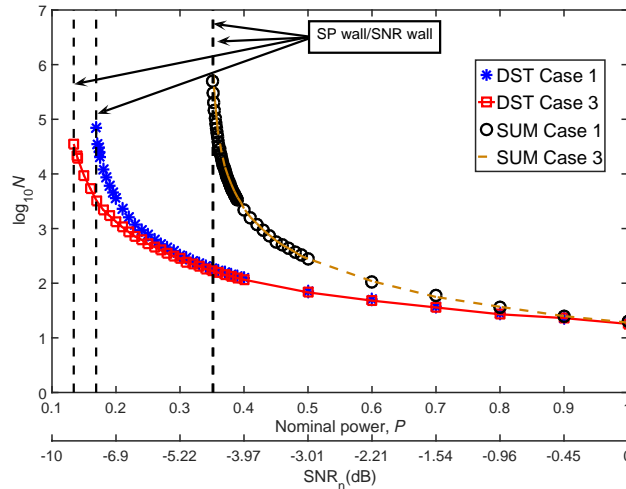


Figure 5.12: Comparison of the DST and sum fusion rules in terms of sample size N as a function of P and $\text{SNR}_n(\text{dB})$ with NU parameters corresponding to cases I and III in Table 5.1 with $\sigma_{ni}^2 = \sigma_n^2$.

Figs. 5.12 and 5.13 show the comparison between the received signal sample size N (log scale) vs nominal signal power P for sum and DST based CED schemes. While Fig. 5.12 shows the plots for NU parameters corresponding to cases I and III of Table 5.1, where $\sigma_{ni}^2 = \sigma_n^2$, making it possible to use $\text{SNR}_n(\text{dB})$ in addition to P as visible from the figure. On the other hand, Fig. 5.13 shows the plot for NU parameters corresponding to cases II and IV of Table 3.1, where $\sigma_{ni}^2 \neq \sigma_n^2$, making it impossible to use $\text{SNR}_n(\text{dB})$ in addition to P as visible from the figure. It can be clearly observed from both the figures that the DST based CED scheme is able to significantly lower the sample size to achieve the same detection performance of $P_{fa} \leq 0.1$ and $P_d \geq 0.9$ at the FC. Moreover, the value of SP_{wall} for the proposed DST based CED is much lower than that of traditional sum rule in all the considered scenarios.

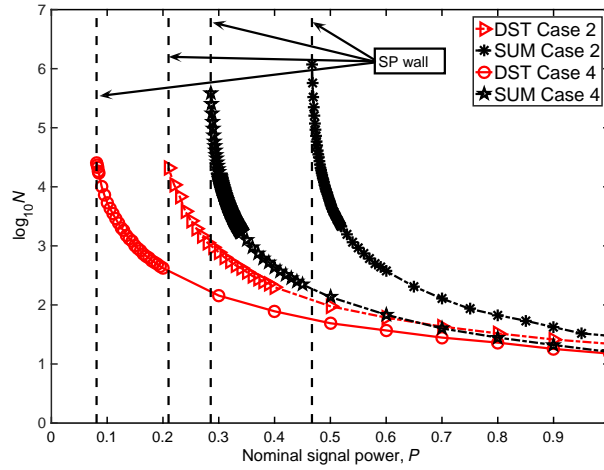


Figure 5.13: Comparison of the DST and sum fusion rules in terms of sample size N as a function of P for scenarios corresponding to cases II and IV in Table 5.1.

Chapter 6

Conclusion

Two NU models has been considered in this thesis. First NU model considered noise power as an unknown but deterministic constant lying within a lower and an upper bound. These bounds define the NU interval and are obtained using the nominal noise variance and the uncertainty factor, which we assume is known to us. For the heterogeneous CR network, the nominal noise variances and uncertainty values will be dissimilar for different CR nodes. In the second NU model, noise variance is assumed to be a random variable having a known distribution.

The outcome of this thesis can be categorized into two main parts. The first part gives the generalized SNR wall which has been termed as signal power wall or SP wall in short. The SP wall expression is obtained by considering the first model of noise variance, i.e., as an unknown but deterministic constant. The idea of SP wall comes into picture when we consider all the participating nodes present in the CR network to be heterogeneous in nature, i.e., having different NU parameters. All other forms of SNR walls for homogeneous or single CR node can be obtained from the generalized SP wall expression. We also noticed that in case of CSS using traditional soft combining fusion rule, the cooperation does not contribute in lowering the SNR wall for ED. In fact the SNR wall for an ED and that of CED is identical. However, when the nominal SNR is greater than the SNR wall, cooperation does help in reducing the sample size N at individual SU for achieving the same detection performance.

In the second part of the thesis, two DST based CED schemes were proposed depending on the NU model used. A new BMA method is introduced based on energy of the received signal. As already mentioned before, depending upon the NU model used we have two slightly different BMA techniques, which basically differentiates the two schemes. However, the combining rule remains the same for both of them, which is Dempster rule of combination.

In the absence of NU, we observed that the performance of proposed DST based CED test statistic is same as the LRT. The proposed DST based CED approach can also incorporate the uncertainty in the noise variance by discounting the BMA from each SU by a rate proportional to the amount of uncertainty in the noise variance at that SU. The performance of DST was compared to that of the traditional sum fusion rule. It was shown that the DST fusion rule performs similar to the sum fusion rule in the absence of NU. In the presence of NU, the proposed DST fusion rule significantly outperforms the sum

fusion rule in terms of detection performance and location of SP wall for different considered scenarios of heterogeneity in NU parameters.

Future work: DST offers new possibilities and opens different dimensions to tackle uncertainty in observed data. Decision making based on DST can be applied to many different fields and applications where uncertainty is a dominant issue. Extension of DST to topics related to wireless sensor networks, heterogeneous sensor data fusion sounds interesting and can be explored further.

Related Publications

Journal Article:

1. P. B. Gohain, S. Chaudhari and V. Koivunen “Cooperative Energy Detection with Heterogeneous Sensors under Noise Uncertainty: Generalized SNR Wall and use of Evidence Theory,” submitted to *IEEE Transactions on Cognitive Communications and Networking*, June 2017.

Conference Papers:

1. P. B. Gohain, S. Chaudhari and V. Koivunen “Evidence Theory based Cooperative Energy Detection under Noise Uncertainty,” accepted in *IEEE Global Communications Conference (GLOBECOM)*, Singapore, Dec. 4-8, 2017.
2. P. B. Gohain and S. Chaudhari, “Cooperative Energy Detection using Dempster-Shafer Theory under Noise Uncertainties,” accepted in *9th IEEE International Conference on COMMunication Systems & NETWORKS (COMSNETS)*, Bangalore, India, Jan. 4-8, 2017.

Bibliography

- [1] R. H. Coase, “The Federal Communications Commission,” *The Journal of Law and Economics*, vol. 2, pp. 1–40, Oct, 1959.
- [2] NTIA, “US frequency allocation chart,” 2003.
Online: <https://www.ntia.doc.gov/files/ntia/publications/2003-allochrt.pdf>.
- [3] M. R. Palattella, M. Dohler, A. Grieco, G. Rizzo, J. Torsner, T. Engel, and L. Ladid, “Internet of things in the 5G era: Enablers, architecture, and business models,” *IEEE Journal on Selected Areas in Communications*, vol. 34, pp. 510–527, March 2016.
- [4] W. Ejaz, A. Anpalagan, M. A. Imran, M. Jo, M. Naeem, S. B. Qaisar, and W. Wang, “Internet of things (iot) in 5G wireless communications,” *IEEE Access*, vol. 4, pp. 10310–10314, 2016.
- [5] X. Shen, “Device-to-device communication in 5g cellular networks,” *IEEE Network*, vol. 29, pp. 2–3, March 2015.
- [6] S. Chen, R. Ma, H. H. Chen, H. Zhang, W. Meng, and J. Liu, “Machine-to-machine communications in ultra-dense networks – a survey,” *IEEE Communications Surveys Tutorials*, vol. PP, no. 99, pp. 1–1, 2017.
- [7] S. Chaudhari, *Spectrum sensing for cognitive radios: Algorithms, performance, and limitations*. PhD thesis, School of Electrical Engineering, Aalto University Finland, Nov. 2012.
- [8] V. T. Nguyen, N. Nguyen-Thanh, L. Yang, D. H. N. Nguyen, C. Jabbour, and B. Murmann, “Cognitive computation and communication: A complement solution to cloud for IoT,” in *International Conference on Advanced Technologies for Communications (ATC)*, pp. 222–230, Oct 2016.
- [9] A. Aijaz and A. H. Aghvami, “Cognitive machine-to-machine communications for internet-of-things: A protocol stack perspective,” *IEEE Internet of Things Journal*, vol. 2, pp. 103–112, April 2015.
- [10] E. Biglieri, A. Goldsmith, L. Greenstein, V. Poor, and B. Mandayam, *Principles of Cognitive Radio*. Cambridge University Press, 2013.

- [11] I. F. Akyildiz, W.-Y. Lee, M. C. Vuran, and S. Mohanty, "Next generation/dynamic spectrum access/cognitive radio wireless networks: A survey," *Computer networks*, vol. 50, no. 13, pp. 2127–2159, 2006.
- [12] X. Hong, J. Wang, C.-X. Wang, and J. Shi, "Cognitive radio in 5g: a perspective on energy-spectral efficiency trade-off," *IEEE Communications Magazine*, vol. 52, no. 7, pp. 46–53, 2014.
- [13] C.-I. Badoi, N. Prasad, V. Croitoru, and R. Prasad, "5g based on cognitive radio," *Wireless Personal Communications*, vol. 57, no. 3, pp. 441–464, 2011.
- [14] P. Rawat, K. D. Singh, and J. M. Bonnin, "Cognitive radio for m2m and internet of things: A survey," *Computer Communications*, vol. 94, pp. 1–29, 2016.
- [15] A. Aijaz and A. H. Aghvami, "Cognitive machine-to-machine communications for internet-of-things: A protocol stack perspective," *IEEE Internet of Things Journal*, vol. 2, no. 2, pp. 103–112, 2015.
- [16] M. A. Shah, S. Zhang, and C. Maple, "Cognitive radio networks for internet of things: Applications, challenges and future," in *Automation and Computing (ICAC), 2013 19th International Conference on*, pp. 1–6, IEEE, 2013.
- [17] S. Haykin, D. J. Thomson, and J. H. Reed, "Spectrum sensing for cognitive radio," *Proceedings of the IEEE*, vol. 97, pp. 849–877, May 2009.
- [18] E. Axell, G. Leus, E. G. Larsson, and H. V. Poor, "Spectrum sensing for cognitive radio : State-of-the-art and recent advances," *IEEE Signal Processing Magazine*, vol. 29, pp. 101–116, May 2012.
- [19] S. Maleki, A. Pandharipande, and G. Leus, "Energy-efficient distributed spectrum sensing for cognitive sensor networks," *IEEE Sensors Journal*, vol. 11, pp. 565–573, March 2011.
- [20] D. M. M. Plata and Á. G. A. Reátiga, "Evaluation of energy detection for spectrum sensing based on the dynamic selection of detection-threshold," *Procedia Engineering*, vol. 35, pp. 135–143, 2012.
- [21] S. Atapattu, C. Tellambura, and H. Jiang, "Energy detection based cooperative spectrum sensing in cognitive radio networks," *IEEE Transactions on Wireless Communications*, vol. 10, pp. 1232–1241, April 2011.
- [22] J. Ma, G. Zhao, and Y. Li, "Soft combination and detection for cooperative spectrum sensing in cognitive radio networks," *IEEE Transactions on Wireless Communications*, vol. 7, pp. 4502–4507, November 2008.

- [23] B. Shent, L. Huang, C. Zhao, Z. Zhou, and K. Kwak, "Energy detection based spectrum sensing for cognitive radios in noise of uncertain power," in *2008 International Symposium on Communications and Information Technologies*, pp. 628–633, Oct 2008.
- [24] R. Tandra and A. Sahai, "SNR walls for signal detection," *IEEE Journal of Selected Topics in Signal Processing*, vol. 2, pp. 4–17, Feb 2008.
- [25] J. Zeng and X. Su, "On SNR wall phenomenon under cooperative energy detection in spectrum sensing," in *2015 10th International Conference on Communications and Networking in China (ChinaCom)*, pp. 53–60, Aug 2015.
- [26] Z. Li, X. Su, J. Zeng, Y. Kuang, and H. Wang, "A study of SNR wall phenomenon under cooperative energy spectrum sensing," in *2013 22nd International Conference on Computer Communication and Networks (ICCCN)*, pp. 1–5, July 2013.
- [27] G. Shafer, *A Mathematical Theory of Evidence*. Princeton university press, 1976.
- [28] L. Zadeh, "A simple view of the Dempster-Shafer theory of evidence and its implication for the rule of combination," *AI Mag.*, vol. 7, pp. 85–90, July 1986.
- [29] U. Rakowsky, "Fundamentals of the Dempster-Shafer theory and its applications to system safety and reliability modelling," in *Reliab. Theory Appl.*, no. 3, pp. 173–185, 2007.
- [30] L. Liu and R. Yager, *Classic Works of the Dempster-Shafer Theory of Belief Functions: An Introduction*, pp. 1–34. Berlin, Heidelberg: Springer Berlin Heidelberg, 2008.
- [31] Z. Quan, S. Cui, and A. H. Sayed, "Optimal linear cooperation for spectrum sensing in cognitive radio networks," *IEEE Journal of selected topics in signal processing*, vol. 2, no. 1, pp. 28–40, 2008.
- [32] E. Drakopoulos and C. Lee, "Decision rules for distributed decision networks with uncertainties," *IEEE Transactions on Automatic Control*, vol. 37, pp. 5–14, Jan 1992.
- [33] P. Qihang, Z. Kun, W. Jun, and L. Shaoqian, "A distributed spectrum sensing scheme based on credibility and evidence theory in cognitive radio context," in *IEEE 17th International Symposium on Personal, Indoor and Mobile Radio Communications*, pp. 1–5, Sept 2006.
- [34] N. Nguyen-Thanh and I. Koo, "An enhanced cooperative spectrum sensing scheme based on evidence theory and reliability source evaluation in cognitive radio context," *IEEE Communications Letters*, vol. 13, pp. 492–494, July 2009.
- [35] N. N. Thanh and I. Koo, "Evidence-theory-based cooperative spectrum sensing with efficient quantization method in cognitive radio," *IEEE Transactions on Vehicular Technology*, vol. 60, pp. 185–195, Jan 2011.

- [36] K. Hamdi, X. N. Zeng, A. Ghayeb, and K. B. Letaief, "Impact of noise power uncertainty on cooperative spectrum sensing in cognitive radio systems," in *IEEE Global Communications Conference (GLOBECOM)*, pp. 1–5, Dec 2010.
- [37] H. Wang, Y. Xu, X. Su, and J. Wang, "Cooperative spectrum sensing in cognitive radio under noise uncertainty," in *2010 IEEE 71st Vehicular Technology Conference*, pp. 1–5, May 2010.
- [38] B. A. Fette, *Cognitive radio technology*. Academic Press, 2009.
- [39] J. Mitola and G. Q. Maguire, "Cognitive radio: making software radios more personal," *IEEE personal communications*, vol. 6, no. 4, pp. 13–18, 1999.
- [40] J. Mitola, "Cognitive radio—an integrated agent architecture for software defined radio," 2000.
- [41] S. Haykin, "Cognitive radio: brain-empowered wireless communications," *IEEE journal on selected areas in communications*, vol. 23, no. 2, pp. 201–220, 2005.
- [42] I. F. Akyildiz, W.-Y. Lee, M. C. Vuran, and S. Mohanty, "Next generation/dynamic spectrum access/cognitive radio wireless networks: A survey," *Computer networks*, vol. 50, no. 13, pp. 2127–2159, 2006.
- [43] FCC, "FCC notice of proposed rule making and order: Facilitating opportunities for flexible, efficient, and reliable spectrum user employing cognitive radio technologies et docket no. 03-108," Feb. 2005.,"
- [44] M. Mouly, M.-B. Pautet, and T. Foreword By-Haug, *The GSM system for mobile communications*. Telecom publishing, 1992.
- [45] L. Korowajczuk, *LTE, WiMAX and WLAN network design, optimization and performance analysis*. John Wiley & Sons, 2011.
- [46] A. M. Wyglinski, M. Nekovee, and T. Hou, *Cognitive radio communications and networks: principles and practice*. Academic Press, 2009.
- [47] S. Geirhofer, L. Tong, and B. M. Sadler, "Cognitive radios for dynamic spectrum access - dynamic spectrum access in the time domain: Modeling and exploiting white space," *IEEE Communications Magazine*, vol. 45, pp. 66–72, May 2007.
- [48] J. Mitola, "Software radios: Survey, critical evaluation and future directions," *IEEE Aerospace and Electronic Systems Magazine*, vol. 8, no. 4, pp. 25–36, 1993.
- [49] Q. Zhao and B. M. Sadler, "A survey of dynamic spectrum access," *IEEE Signal Processing Magazine*, vol. 24, pp. 79–89, May 2007.

- [50] M. L. D. Ariananda and H. Nikoo, "A survey on spectrum sensing techniques for cognitive radio," *Proc. of the International Workshop on Cognitive Radio and Advanced Spectrum Management (CogART)*, pp. 74–79, 2009.
- [51] T. Yucek and H. Arslan, "A survey of spectrum sensing algorithms for cognitive radio applications," *IEEE Communications Surveys Tutorials*, vol. 4, no. 1, pp. 116–130, 2011.
- [52] I. F. Akyildiz, W.-Y. Lee, M. C. Vuran, and S. Mohanty, "Next generation/dynamic spectrum access/cognitive radio wireless networks: A survey," *Computer networks*, vol. 50, no. 13, pp. 2127–2159, 2006.
- [53] W. A. Gardner, A. Napolitano, and L. Paura, "Cyclostationarity: Half a century of research," *Signal Process.*, vol. 86, pp. 639–697, Apr. 2006.
- [54] W. A. Gardner, A. Napolitano, and L. Paura, "Cyclostationarity: Half a century of research," *Signal processing*, vol. 86, no. 4, pp. 639–697, 2006.
- [55] E. Serpedin, F. Panduru, I. Sari, and G. B. Giannakis, "Bibliography on cyclostationarity," *Signal Processing*, vol. 85, no. 12, pp. 2233–2303, 2005.
- [56] J. Lundén, V. Koivunen, A. Huttunen, and H. V. Poor, "Collaborative cyclostationary spectrum sensing for cognitive radio systems," *IEEE Transactions on Signal Processing*, vol. 57, no. 11, pp. 4182–4195, 2009.
- [57] M. A. Abdulsattar and Z. A. Hussein, "Energy detector with baseband sampling for cognitive radio: Real-time implementation," *Wireless Engineering and Technology*, vol. 3, no. 04, p. 229, 2012.
- [58] P. K. Varshney, *Distributed detection and data fusion*. Springer Science & Business Media, 2012.
- [59] S. A. Kassam, *Signal detection in non-Gaussian noise*. Springer Science & Business Media, 2012.
- [60] H. V. Poor, *An introduction to signal detection and estimation*. Springer Science & Business Media, 2013.
- [61] G. Ganesan and Y. Li, "Cooperative spectrum sensing in cognitive radio networks," in *First IEEE International Symposium on New Frontiers in Dynamic Spectrum Access Networks, 2005. DySPAN 2005.*, pp. 137–143, Nov 2005.
- [62] Z. Li, F. R. Yu, and M. Huang, "A distributed consensus-based cooperative spectrum-sensing scheme in cognitive radios," *IEEE Transactions on Vehicular Technology*, vol. 59, pp. 383–393, Jan 2010.
- [63] J. Unnikrishnan and V. V. Veeravalli, "Cooperative sensing for primary detection in cognitive radio," *IEEE Journal of selected topics in signal processing*, vol. 2, no. 1, pp. 18–27, 2008.

- [64] A. Ghasemi and E. S. Sousa, "Collaborative spectrum sensing for opportunistic access in fading environments," in *New Frontiers in Dynamic Spectrum Access Networks, 2005. DySPAN 2005. 2005 First IEEE International Symposium on*, pp. 131–136, IEEE, 2005.
- [65] Z. Li, F. R. Yu, and M. Huang, "A cooperative spectrum sensing consensus scheme in cognitive radios," in *INFOCOM 2009, IEEE*, pp. 2546–2550, IEEE, 2009.
- [66] W. Zhang and K. B. Letaief, "Cooperative spectrum sensing with transmit and relay diversity in cognitive radio networks-[transaction letters]," *IEEE Transactions on Wireless Communications*, vol. 7, no. 12, 2008.
- [67] G. Ganesan and Y. Li, "Cooperative spectrum sensing in cognitive radio, part ii: multiuser networks," *IEEE Transactions on wireless communications*, vol. 6, no. 6, pp. 2214–2222, 2007.
- [68] P. K. Varshney, *Distributed detection and data fusion*. Springer Science & Business Media, 2012.
- [69] P. K. Varshney, *Distributed detection and data fusion*. Springer Science & Business Media, 2012.
- [70] R. Viswanathan and P. K. Varshney, "Distributed detection with multiple sensors part i. fundamentals," *Proceedings of the IEEE*, vol. 85, no. 1, pp. 54–63, 1997.
- [71] S. Chaudhari, J. Lunden, V. Koivunen, and H. V. Poor, "Cooperative sensing with imperfect reporting channels: Hard decisions or soft decisions?," *IEEE transactions on signal processing*, vol. 60, no. 1, pp. 18–28, 2012.
- [72] S. Kay, *Fundamental of Statistical Signal Processing: Volume II Detection Theory*. Prentice Hall, 1998.
- [73] B. Gendenko and A. Kolmogoro, "Limit distributions for sums of independent random variables," *Reading, MA: Addison-Wesley*, 1954.
- [74] R. Umar, A. U. H. Sheikh, and M. Deriche, "Unveiling the hidden assumptions of energy detector based spectrum sensing for cognitive radios," *IEEE Communications Surveys Tutorials*, vol. 16, pp. 713–728, Second 2014.
- [75] S. Kay, *Fundamental of Statistical Signal Processing: Volume I Estimation Theory*. Prentice Hall, 1998.
- [76] A. P. Dempster, "Upper and lower probabilities induced by a multivalued mapping," *Ann. Math. Statist.*, vol. 38, pp. 325–339, 04 1967.
- [77] A. P. Dempster, "Upper and lower probabilities generated by a random closed interval," in *Annals of Mathematical Statistics* 39, pp. 957–966, 1968.
- [78] A. P. Dempster, "Upper and lower probabilities inferences for families of hypothesis with monotone density ratios," in *Annals of Mathematical Statistics* 40, pp. 953–969, 1969.

- [79] T. Denœux, “Conjunctive and disjunctive combination of belief functions induced by nondistinct bodies of evidence,” *Artificial Intelligence*, vol. 172, no. 2, pp. 234 – 264, 2008.
- [80] A. Dempster, “The Dempster–Shafer calculus for statisticians,” *International Journal of Approximate Reasoning*, vol. 48, no. 2, pp. 365 – 377, 2008.